Received: 7 August 2025 | Accepted: 15 March 2026

DOI: 10.1111/1365-2435.70341

Functional Ecology

RESEARCH ARTICLE

Depth-dependent mechanisms regulate accumulation of plant- and microbial-derived residues under long-term nitrogen addition in a semiarid grassland

Xiaobo Yuan[1] | Shize Yao[1] | Guiyao Zhou[2,3] | Adam Frew[4,5,6] | Peter Dietrich[7,8] | Yuan Li[9] | Ying Wang[10] | Tian Ma[11] | Ning Chen[12,13] | Yaodan Zhang[1] | Jingrun Xu[1] | Shujuan Wu[1] | Mengfei Zhang[1] | Yaodong Li[1] | Baoming Du[14] | Peijing Chang[15] | Tianhu Han[1,10] | Decao Niu[1] | Hua Fu[1] | Zengru Wang[1]

[1]State Key Laboratory of Herbage Improvement and Grassland Agroecosystems, Key Laboratory of Grassland Livestock Industry Innovation, Ministry of Agriculture and Rural Affairs, Engineering Research Center of Grassland Industry, Ministry of Education, College of Pastoral Agriculture Science and Technology, Lanzhou University, Lanzhou, People's Republic of China; [2]Laboratorio de Biodiversidady Funcionamiento Ecosistémico, Instituto de Recursos Naturales y Agrobiología de Sevilla (IRNAS), CSIC, Sevilla, Spain; [3]German Centre for Integrative Biodiversity Research (iDiv) Halle-Jena-Leipzig, Leipzig, Germany; [4]Hawkesbury Institute for the Environment, Western Sydney University, Penrith, New South Wales, Australia; [5]Centre for Crop Health, University of Southern Queensland, Toowoomba, Queensland, Australia; [6]Department of Biological and Environmental Sciences, University of Jyväskylä, Jyväskylän yliopisto, Finland; [7]German Centre of Integrative Biodiversity Research (iDiv)Halle-Jena-Leipzig, Leipzig, Germany; [8]Institute of Biology, Leipzig University, Leipzig, Germany; [9]Grassland and Sustainable Farming Production Systems, Natural Resources Institute Finland, Maaninka, Finland; [10]Linze Desert Ecosystem Research Station, Gansu Desert Control Research Institute, Lanzhou, People's Republic of China; [11]CAS Key Laboratory of Coastal Zone Environmental Processes and Ecological Remediation, Yantai Institute of Coastal Zone Research, Chinese Academy of Sciences, Yantai, Shandong, China; [12]State Key Laboratory of Herbage Improvement and Grassland Agro-Ecosystems, College of Ecology, Lanzhou University, Lanzhou, People's Republic of China; [13]Yuzhong Mountain Ecosystem Observation and Research Station, Lanzhou University, Lanzhou, People's Republic of China; [14]School of Agriculture and Biology, Shanghai Jiao Tong University, Shanghai, People's Republic of China and [15]Alxa League Meteorological Bureau, Bayanhaote, People's Republic of China

Correspondence
Xiaobo Yuan
Email: yuanxb@lzu.edu.cn

Zengru Wang
Email: wangzengru@lzu.edu.cn

Funding information
National Key Research and Development Program of China, Grant/Award Number: 2023YFF0806800; National Natural Science Foundation of China, Grant/Award Number: 32101445; Natural Science Foundation of Gansu Province of China, Grant/Award Number: 22JR5RA467; Initial Funding of Scientific Research for Imported Talents of Lanzhou University, Grant/Award Number: 561121201; Alxa League Science and Technology Program, Grant/Award Number: AMYY2022-16

Handling Editor: Sandra Varga

Abstract

1. Plant- and microbial-derived residues constitute the primary sources of soil organic carbon (SOC) in grassland ecosystems. However, their differential responses to chronic nitrogen (N) enrichment and the depth-dependent mechanisms governing their accumulation remain poorly characterized, particularly for water-limited grassland systems.
2. Based on a 13-year field experiment in a semiarid grassland, we quantified the effects of long-term N addition on the accumulation of plant- (lignin phenols) and microbial-derived (amino sugars) residues.
3. We found that N addition significantly increased lignin phenol content and its contribution to SOC in the topsoil, whereas lignin phenols exhibited a hump-shaped response peaking under moderate N levels in the subsoil. Amino sugar concentrations and their relative contribution to SOC increased in both soil layers under N addition but declined at the highest N input. The dominant factors regulating residue accumulation varied with soil depth: in the topsoil, microbial *K*–/*r*-traits and community composition primarily explained lignin phenol and amino

sugar dynamics, while in the subsoil, mineral-associated protection and microbial composition were the key drivers.
4. These findings underscore the depth-dependent nature of SOC formation pathways and highlight the importance of incorporating both plant- and microbial-derived residues into Earth System Models to improve projections of carbon-climate feedback under changing nitrogen regimes.

KEYWORDS
amino sugars, lignin phenols, microbial *K*-/*r*-traits, microbial residues, mineral protection, nitrogen deposition

1 | INTRODUCTION

Soil organic carbon (SOC) represents the largest carbon (C) reservoir in the terrestrial biosphere, with approximately 1500 Pg (1 Pg = 10^{15} g) C stored within the top meter of soil (Balesdent et al., 2018; Carvalhais et al., 2014; Crowther, van den Hoogen, et al., 2019). Even small changes in this C pool can trigger substantial feedbacks—either amplifying or mitigating—on climate warming (Liu et al., 2022; Schuur et al., 2015). In recent decades, intensified human activities such as agricultural expansion and fossil fuel combustion have significantly increased reactive nitrogen (N) inputs and deposition into terrestrial ecosystems (Galloway et al., 2008). These N inputs influence not only nutrient cycling but also key ecosystem functions, including C sequestration (Hu, Deng, et al., 2024; Janssens et al., 2010; Neff et al., 2002; Pastore et al., 2021). In general, moderate N inputs may stimulate plant growth and soil nutrient cycling in grasslands, thereby enhancing soil C sequestration (Zhang, Niu, et al., 2025). However, excessive N supply can cause plant nutrient imbalances and soil acidification, which inhibit plant communities and biodiversity, ultimately reducing soil C sequestration (Chen et al., 2018; Knorr et al., 2024; Yang et al., 2024). While short-term responses of soil C stocks to N addition are relatively well understood (Chen et al., 2018; Hu, Deng, et al., 2024), a comprehensive understanding of how long-term N enrichment affects SOC in terrestrial ecosystems remains lacking (Crowther, Riggs, et al., 2019; Pastore et al., 2021; Ye et al., 2018). It remains unclear whether long-term N enrichment induces a nonlinear response in SOC dynamics and through which mechanisms such changes might occur. Such knowledge is critical for improving projections of changes in terrestrial C sink capacity under ongoing global change.

SOC has traditionally been considered as deriving mainly from chemically recalcitrant structural compounds in plant residues (Angst et al., 2021, 2025; Schmidt et al., 2011) and from root exudates (Wilson et al., 2018). However, recent advances in the 'microbial carbon pump' concept highlight the crucial role of microbial-derived residues in SOC formation and stabilization (Feng & Wang, 2023; Liang et al., 2017; Schmidt et al., 2011), as these residues are more readily stabilized within soil aggregates and mineral associations (Cotrufo et al., 2013; Kallenbach et al., 2016; Liang et al., 2017; Sokol et al., 2022). Despite microbial residues contributing up to 50% of SOC in grasslands (Liang et al., 2019; Wang et al., 2021), the relative contributions of plant- and microbial-derived residues remain debated, likely due to ecosystem-specific controls and interacting biotic and abiotic factors (Angst et al., 2021; Liang et al., 2019; Whalen et al., 2022). Generally, the quantity and quality of plant residues directly influence growth, turnover and carbon use efficiency of microbes (Cotrufo et al., 2013; Domeignoz-Horta et al., 2024; Prommer et al., 2020; Zeng et al., 2022), thereby shaping the formation and persistence of microbial residues in soils (Cotrufo et al., 2022; Craig et al., 2022; Whalen et al., 2022). However, interpreting microbial contributions based solely on metabolic traits ignores taxonomic specificity and interspecies interactions, which also influence the stabilization of both plant- and microbial-derived residues (Liu, Zhao, et al., 2025; Yang et al., 2024; Zhang, Niu, et al., 2025). The ecological *r*/*K* selection framework offers further insight: fast-growing r-strategists (copiotrophs) dominate in environments rich in labile substrates, whereas slow-growing *K*-strategists (oligotrophs) are better adapted to utilizing recalcitrant C sources (Fierer et al., 2007). This framework can be extended to functional genes involved in labile and recalcitrant C degradation, enhancing predictions of SOC dynamics (Li et al., 2021; Zeng et al., 2022). Moreover, microbial communities form complex co-occurrence networks, with taxa sharing similar resource niches clustering into ecological modules that mediate SOC turnover and stabilization (Guseva et al., 2022; Liao et al., 2022; Yuan et al., 2021; Zhang, Niu, et al., 2025). N enrichment adds an additional layer of complexity by altering microbial diversity (Hu, Delgado-Baquerizo, et al., 2024; Zhou et al., 2020), shifting r/K strategist balances (Carson & Zeglin, 2018; Yang et al., 2024) and reorganizing network structure (Liu, Yang, et al., 2025; Ma, Wang, et al., 2022; Zhang, Niu, et al., 2025). Yet, it remains unclear how these microbial shifts collectively regulate the accumulation and stabilization of plant- and microbial-derived residues under long-term N addition, and how this shapes SOC persistence.

Emerging evidence suggests that SOC responses to N addition are strongly modulated by depth-dependent soil and microbial properties (Hu, Deng, et al., 2024). In subsoils, where plant C inputs via litter deposition are limited and C derives primarily from root litter and rhizodeposits (Chen et al., 2021; He et al., 2022), increased mineral protection, lower nutrient availability and reduced oxygen availability, microbial composition differs and growth is suppressed, which affects the accumulation of plant- and microbial-derived residues and their contributions to SOC (He et al., 2022; Huang et al., 2023; Liu et al., 2023).

For instance, microbial life-history strategies progressively shift from copiotrophs (*r*-strategists) that favour organic-rich environments to oligotrophs (*K*-strategists) adapted to nutrient-depleted mineral soils along the soil profile (Christiansen et al., 2025; Jílková et al., 2025). Consistent with these shifts, subsoils exhibit a lower proportion of plant-derived residues and a higher proportion of microbial residues, which are more strongly bound to mineral surfaces (Angst et al., 2021; Huang et al., 2023; Liu et al., 2023). These depth-dependent contrasts indicate that the processes governing the formation and turnover of plant- and microbial-derived residues in subsoils under long-term N addition are likely to differ from those of surface soils. However, we still lack a mechanistic understanding of (i) how long-term N enrichment regulates the relative contributions of plant- and microbial-derived residues to SOC at different soil depths and (ii) how depth-specific plant inputs, microbial traits and mineral protection interact to control the accumulation and stabilization of these residues. Addressing this gap is especially important in arid and semiarid grasslands, where both plant and microbial communities are co-limited by nutrients and water, and where subsoils store a substantial but understudied fraction of SOC (Balesdent et al., 2018; Peng et al., 2025). Against this background, a depth-explicit comparison of plant- and microbial-derived residues under chronic N loading represents a promising and innovative direction for advancing our understanding of SOC persistence.

Based on an existing 13-year N addition experiment in a semiarid grassland on the Loess Plateau (northwestern China), this study aimed to determine how long-term N enrichment affects plant- and microbial-derived residues contribute to SOC accumulation across soil depths. Soil samples were collected from two depths (0–10 cm topsoil and 10–20 cm subsoil), and lignin phenols and amino sugars quantified as tracers of plant- and microbial-derived C inputs, respectively. To identify the key factors controlling the accumulation of these residues, we measured a range of biotic and abiotic variables including plant carbon inputs, soil physicochemical properties, mineral-associated protection and microbial traits such as community composition, *K*-/*r*-strategist characteristics and co-occurrence network structures. We specifically hypothesized that: (i) N addition would promote the accumulation of both plant-derived lignin phenols and microbial-derived amino sugars, with microbial residues contributing more substantially to SOC formation; and (ii) the key drivers of residue accumulation differ with soil depth, whereby topsoil residues are primarily co-regulated by plant C inputs and microbial traits, whereas subsoil residues are more strongly influenced by microbial characteristics and mineral protection.

2 | MATERIALS AND METHODS

2.1 | Site description and experimental design

This study was carried out at the Semiarid Climate and Environment Observatory of Lanzhou University (SACOL; 104°09′ E, 35°57′ N, 1966 m a.s.l.) on the northwestern Loess Plateau, China. The region has a continental semiarid climate, with a mean annual precipitation of 383.8 mm and a mean annual temperature of 6.8°C (Yuan, Niu, Wang, et al., 2019; Zhang, Niu, et al., 2025). Soil type is sierozem according to the US soil taxonomy classification (Li et al., 2010). Vegetation is dominated by the perennial bunchgrass *Stipa bungeana* (Niu et al., 2018; Xu et al., 2024; Zhang, Wang, et al., 2025). The annual atmospheric N deposition in the experimental area ranges from approximately 1 to 1.70 g N m^{-2} $year^{-1}$ (Chen et al., 2023).

The experimental design has been described previously by Yuan et al. (2020, 2023). In brief, 30 plots of six treatments with five replicates were arranged in a completely randomized design in May 2009. Each plot was 4 m × 5 m and separated by a 0.5 m buffer strip. N was added as urea [$CO(NH_2)_2$] solution at six N-addition levels (N_{rate}): N_0, $N_{1.15}$, $N_{2.30}$, $N_{4.60}$, $N_{9.20}$, $N_{13.80}$, corresponding to 0, 1.15, 2.30, 4.60, 9.20 and 13.80 g N m^{-2} $year^{-1}$, respectively. N was applied twice each year, with half the annual amount added in late May and the remainder in late June. For each application, urea was dissolved in 10 L of purified water and uniformly applied to the plots with a portable sprayer on rainy days. Control plots were treated with 10 L of purified water. Previous studies conducted at this experimental site have shown that N addition significantly increases plant aboveground biomass (Niu et al., 2018), decreases plant species richness and Shannon diversity (Yuan et al., 2020), and alters soil microbial community structure and function as well as SOC content in the surface soil (Xu et al., 2024; Yuan et al., 2023; Zhang, Niu, et al., 2025; Zhang, Wang, et al., 2025).

2.2 | Plant and soil sampling

To assess the effects of plant C inputs on the accumulation of both plant-derived lignin phenols and microbial-derived amino sugars at different soil layers under N addition, we measured above-ground, litter and below-ground biomass in each plot during the peak growing season (mid-August 2021). In each plot, a 1 m × 1 m quadrat was placed randomly (Xu et al., 2024; Zhang, Niu, et al., 2025). Within each quadrat, above-ground biomass was harvested by cutting off at ground level, after which litter was collected. Below-ground biomass was determined by extracting two soil cores (12.5 cm in inner diameter) from each quadrat at soil depths of 0–10 cm (topsoil) and 10–20 cm (subsoil). All plant materials were oven-dried at 70°C for 48 h to determine their dry weight (g m^{-2}).

Soil samples were collected from each quadrat at five points along a diagonal transect using a soil auger (7.5 cm inner diameter) for both topsoil and subsoil. Soil samples from each plot and depth were homogenized and passed through a 2 mm sieve to remove roots, plant residues and rocks. Before sampling each plot, the sieve was wiped with 75% ethanol and air-dried to minimize potential cross-contamination of microbes and DNA among plots. The processed soil samples were transported to the laboratory in a portable refrigerator at 4°C. Upon arrival in the laboratory, each soil sample was divided into three subsamples and stored under different conditions: at room temperature for analysis of pH, SOC, mineral properties, lignin phenols and amino sugars; at 4°C for measurements of soil water content, texture (clay and silt), inorganic N, dissolved

organic nutrients, extracellular enzyme activities, microbial biomass and microbial respiration; and at −70°C for DNA extraction and metagenomic analysis.

2.3 | Measurement of soil properties

Soil pH was measured in a 1:2.5 soil-to-water suspension using a glass electrode pH meter (PHS-3C, Shanghai, China). Soil moisture content was determined by oven-drying fresh samples at 105°C for 24 h. Soil texture (clay and silt content) was analysed by laser diffraction after dispersion with sodium hexametaphosphate (Qiu et al., 2021). SOC was analysed with a CHN elemental analyzer (Flash EA1112, Thermo Scientific, FL, USA). Ammonium-N (NH_4^+-N) and nitrate-N (NO_3^--N) were measured using vanadium reduction and the Griess assay, respectively, following extraction with 2 M KCl for 30 min. Total dissolved N (TDN) and soil dissolved organic carbon (DOC) were extracted with 0.5 M K_2SO_4 and quantified using a TOC/TN analyzer (Elementar Vario TOC select, Hanau, Germany). Dissolved organic N (DON) was determined by subtracting inorganic N from TDN (Tapia-Torres et al., 2015).

Exchangeable Ca^{2+} (Ca_{exe}) and Mg^{2+} (Mg_{exe}) were extracted by triethanolamine (pH = 8.1) and 1 M $BaCl_2$, respectively, and quantified by flame atomic absorption spectroscopy (M6AA system, Thermo Scientific, West Palm Beach, FL, USA) (Gruba & Mulder, 2015). The complex Fe/Al oxides (Fe_p and Al_p) were extracted with 0.2 M sodium pyrophosphate solution, while the poorly crystalline Fe/Al oxides (Fe_o and Al_o) were extracted with 0.2 M oxalic acid-ammonium oxalate (pH = 3). Two forms of Fe and Al oxides were determined by inductively coupled plasma-optical emission spectrometry (ICAP 6300, Thermo Scientific, Waltham, MA, USA; Gentsch et al., 2018; Lalonde et al., 2012).

2.4 | Analyses of lignin phenols and amino sugars

Lignin phenols (biomarkers for plant-derived SOC, Angst et al., 2021) were quantified following alkaline CuO oxidation and subsequent gas chromatography, as described by Hedges and Ertel (1982). Briefly, 0.5–1.0 g of dried soil was combined with 1 g CuO, 100 mg ammonium iron (II) sulfate hexahydrate [$Fe(NH4)_2(SO4)_2{\cdot}6H_2O$] and 15 mL of 2 M NaOH (nitrogen-purged) in Teflon vessel. The vessels were flushed with N_2 for 15 min and heated at 150°C for 2.5 h. Lignin oxidation products were supplemented with a recovery standard (ethyl vanillin), centrifuged at 4000 rpm for 3 min, and the supernatant was acidified to pH < 1 with 6 M HCl and kept in the dark for 1 h. Extraction was performed three times with ethyl acetate, and the combined extracts were concentrated under N_2. The dried residues were derivatized with N, O-bis-(trimethylsilyl) trifluoroacetamide (BSTFA) and pyridine (70°C, 3 h) to obtain trimethylsilyl (TMS) derivatives. Lignin phenol derivatives were analysed by gas chromatography (GC; Agilent 6890A, Agilent Technologies) equipped with a TGSil-5MS column (30 m × 0.25 mm × 0.25 μm), using N_2 as carrier gas at a flow rate of 1 mL min^{-1}. The oven temperature was programmed from 65°C (2 min hold) to 300°C at 6°C min^{-1}, with a final hold at 300°C for 20 min; the injector temperature was set to 250°C. Phenols were identified by comparison with the NIST library and quantified against known standards. Total lignin phenol concentrations were calculated as the sum of vanillyl (V)-, syringyl (S)- and cinnamyl (C)-type monomers. Ratios of C/V and S/V, as well as the acid/−aldehyde ratios for V- and S-type phenols ($(Ad/Al)_V$ and $(Ad/Al)_S$) were used to assess the degree of microbial alteration and oxidation of lignin (Chen et al., 2021).

Amino sugars, indicators of microbial residues (Joergensen, 2018), were analysed following the protocol of Zhang and Amelung (1996). In brief, approximately 1.0 g of air-dried soil (sieved to 0.15 mm) was hydrolysed with 6 M HCl at 105°C for 8 h. The hydrolysates solution was supplemented with 100 μg myo-inositol as an internal standard, filtered, neutralized to pH 6.6–6.8 using 0.4 M KOH solution, and centrifuged. Supernatants were freeze-dried, and residues were dissolved in 5 mL methanol, evaporated at 45°C under N_2 and derivatized by incubation with 300 μL of a reagent mixture (hydroxylamine hydrochloride and 4-dimethylaminopyridine in pyridine and methanol, 4:1 v:v) at 80°C for 30 min. Amino sugar derivatives were analysed by gas chromatography (GC; Agilent 6890A, Agilent Technologies). Concentrations of glucosamine (GluN), galactosamine (GalN) and muramic acid (MurN) were determined relative to the internal standard. Total amino sugar content was calculated as the sum of GluN, GalN and MurN. Bacterial residues were estimated from MurN (a bacterial cell wall marker; Angst et al., 2021), while fungal-derived glucosamine was calculated by correcting for the bacterial contribution using a GluN:MurN ratio of 2:1 (Chen et al., 2021; Liang et al., 2019).

2.5 | Soil shotgun metagenomics sequencing

2.5.1 | DNA extraction, metabarcoding and metagenomics library preparation

Total metagenomic DNA was extracted from 0.5 g soil using the FastDNA® SPIN Kit for Soil (MP Biomedicals, OH, USA) according to the manufacturer's instructions and standard laboratory protocol. DNA concentration was measured with a Qubit fluorometer (Thermo Fisher Scientific), and DNA integrity and purity were assessed by 1% agarose gel electrophoresis. All samples used for library preparation had total DNA yields greater than 0.25 ng, with most DNA fragments (smear) above 500 bp and no severe dense bands below 500 bp on agarose gels, and showed no visible impurities or precipitates, discoloration or abnormal viscosity, indicating good integrity and the absence of major degradation or contamination. Only DNA samples that met these quality criteria were used for subsequent metagenomic library construction.

For each soil sample, sequencing libraries were constructed by fragmenting DNA to approximately 350 bp with a Covaris M220 (Covaris, MA, USA), followed by end repair, poly-A tailing, adapter

ligation, purification and PCR amplification. PCR products were purified using the AMPure XP system, and library sizes were checked on an Agilent 2100 Bioanalyzer. Library concentrations were quantified by real-time PCR. Indexed libraries were clustered on a cBot Cluster Generation System using the Illumina PE150 Cluster Kit (Illumina, CA, USA) according to the manufacturer's instructions. Clustered libraries were then sequenced on an Illumina NovaSeq 6000 platform to generate 150 bp paired-end reads.

2.5.2 | Bioinformatic analysis

Metagenomic sequencing of soil fungal and bacterial communities was conducted on the Illumina NovaSeq 6000 high throughput platform, generating paired-end raw reads for each soil sample. To ensure data reliability, raw reads were first subjected to quality control and preprocessing with KneadData as follows: adaptor sequences were removed from the raw bacterial and fungal reads using Trimmomatic (ILLUMINACLIP:adapters_path:2:30:10), and low quality bases were trimmed according to a default quality threshold of $Q \leq 20$ (SLIDINGWINDOW:4:20); reads shorter than 50 bp after trimming were discarded (MINLEN:50). (2) To account for potential host contamination, the clean reads were mapped to the host genome with Bowtie2 (http://bowtie-bio.sourceforge.net/bowtie2/index.shtml), and only unmapped reads were retained as valid sequences for downstream analyses. (3) The effectiveness of the quality control procedure was evaluated using FastQC (Langmead & Salzberg, 2012). Taxonomic assignment was then carried out with Kraken2 against a custom microbial nucleotide database constructed from bacterial and fungal sequences extracted from the NCBI NT nucleotide database and the RefSeq whole genome database, and Bracken was used to estimate the relative abundance of taxa in each soil sample. Kraken2 is a k-mer-based taxonomic classifier, and in this study we used a local Kraken2 database containing 16,799 reference bacterial genomes (Lu et al., 2017). Bracken was used to estimate the relative abundance of microbial taxa within each sample.

2.6 | Soil microbial properties analysis

Microbial biomass carbon (MBC) and N (MBN) were determined using the chloroform fumigation-extraction method (Vance et al., 1987). Microbial respiration was assessed via short-term (7-day) incubations at 20°C, following established protocols (Yuan, Niu, Gherardi, et al., 2019; Zhang, Niu, et al., 2025). Activities of C- and N-acquiring soil enzymes, including β-1,4-glucosidase (BG), β-1,4-N-acetylglucosaminidase (NAG) and leucine aminopeptidase (LAP), were measured in 96-well microplates according to DeForest (2009). The metabolic quotient (qCO_2) was calculated as hourly microbial respiration per unit MBC (μg CO_2-C μg^{-1} MBC h^{-1}; Zeng et al., 2022). Community-scale microbial carbon use efficiency (CUE) was estimated using the biogeochemical equilibrium model described by Sinsabaugh et al. (2016), which has been confirmed to approximate the actual values very accurately. Based on operational taxonomic units (OTUs) abundance tables for fungi and bacteria, taxonomic α-diversity indices (Chao1 estimator and Shannon diversity) were calculated. Effects of N addition on fungal and bacterial community β diversity were evaluated using permutational multivariate analysis of variance (PERMANOVA; *Adonis* function) and unconstrained principal coordinate analysis (PCoA) based on Weighted UniFrac distances in the 'vegan' R package. The first PCoA axis score was used to represent overall shifts in microbial β-diversity induced by N addition.

To explore the influence of N addition on microbial co-occurrence patterns, we performed network analysis using bacterial and fungal phylotypes with an average relative abundance >0.01%, focusing on relatively abundant taxa and reduce spurious associations with rare OTUs (Jiao et al., 2022; Zhang, Wang, et al., 2025). OTUs with Pairwise Spearman correlations (threshold >0.7 and $p < 0.001$) between OTUs were used to construct the network matrix. Main ecological clusters (modules) were identified using the 'igraph' package in R (Csardi, 2013). The absolute abundances of microbes within each module were calculated as described in Zhang, Niu, et al. (2025). Key network topological features including number of nodes and edges, average path length, average degree, clustering coefficient, diameter, density and modularity were determined separately for topsoil and subsoil (Table S1). Network visualization was performed using the *Fruchterman-Reingold* algorithm in Gephi (https://gephi.org). To facilitate further analyses, the absolute abundance data for each major module were standardized using *Z*-score transformation (Figure S1).

Microbial life-history strategies (i.e. *K*-/*r*-traits) were inferred from metagenomic data using the ratio of oligotrophic to copiotrophic taxa and the ratio of genes involved in recalcitrant to labile carbon degradation (R/L genes; Li et al., 2021; Zeng et al., 2022). Relatively abundant bacterial and fungal taxa were assigned to oligotrophic (*K*-strategists) or copiotrophic (*r*-strategists) groups (Table S2). Functional annotation of metagenomes enabled quantification of 15 key genes related to the degradation of lignin (tyrosinase, peroxidase), chitin (mannosyl-glycoprotein endo-β-NAGase and chitinase), aromatics (limonene-1,2-epoxide hydrolase, vanillate monooxygenase), cellulose (cellulase, cellulose 1,4-β-cellobiosidase), hemicelluloses (UDP-arabinopyranose mutase, β-glucosidase, Endo-1,4-β-xylanase) and starch (α-amylase, Glucan 1,4-α-glucosidase, neopullulanase, pullulanase). Further details on gene selection and functional genes classification are provided in Table S3 and Figure S2.

2.7 | Statistical analyses

Normality of residuals (Shapiro–Wilk test) and homogeneity of variance (Levene's test) were checked for all response variables prior to testing treatment effects. All response variables, including

ratio-based metrics, met these assumptions; therefore, no data transformations were applied. Statistical analyses were conducted in three steps. First, one-way analysis of variance (ANOVA) with *Duncan's* post hoc test was used to assess the effects of N addition on the SOC-normalized lignin phenol and amino sugar contents, as well as on the different predictive variables (i.e. plant properties, edaphic condition, mineral protection and microbial properties) in both topsoil and subsoil. Meanwhile, two-way ANOVA were performed to evaluate the effects of N addition, soil depth and their interactions on all measured parameters, with soil depth treated as a within-subject factor and N addition as a between-subject factor.

Second, we examined the relationships of lignin phenols and amino sugars with potential predictors using three commonly used functional forms (linear, exponential and logarithmic) at each soil depth. The potential predictors included edaphic condition (pH, DOC, TDN and DIN), mineral protection (clay + silt, Ca_{exe}, Mg_{exe}, $Fe_p + Al_p$ and $Fe_o + Al_o$), plant C input, microbial metabolism (MBC, MBN, MBC/MBN, qCO_2, CUE, BG, NAG + LAP, BG/NAG + LAP), microbial community composition (fungal community composition, bacterial community composition and main ecological clusters) and microbial K-/r-traits. Model comparisons (Tables S4–S7) showed that most predictor–response relationships were better described by nonlinear functions (i.e. exponential or logarithmic) rather than simple linear relationships. Accordingly, we used Spearman's rank correlation analysis as the primary metric for single-factor associations. We then applied boosted regression tree (BRT) analysis to quantify the relative importance of plant C input, edaphic condition, mineral protection, microbial metabolism, microbial community composition and microbial K-/r-traits on lignin phenol and amino sugar contents within topsoil and subsoil, respectively. While BRT is effective in capturing complex nonlinear relationships and interactions, it does not provide mechanistic inference and may be sensitive to correlated predictors; therefore, results should be interpreted as indicative rather than causal. Significance was set at $p < 0.05$ for all tests.

Third, piecewise structural equation modelling (*piecewise* SEM) was used to further reveal the intricate regulatory pathways of predictive variables on lignin phenol and amino sugar accumulation under N addition for the two soil layers. Only variables significantly affected by N addition and associated with lignin phenol and amino sugar contents were included in the initial model. To address collinearity within mineral protection and microbial properties, principal component analysis (PCA) was performed and the first principal component (PC1; explaining 75.04%–99.16% of the variance) was used to represent each group. When constructing the SEM, we accounted for the nonlinear response of N addition to variables by adding a complex variable composed of N and its quadratic terms. The conceptual model posited that N addition alters plant C input, edaphic condition and soil mineral protection, which in turn affect soil microbial properties and ultimately drive variations in lignin phenol and amino sugar contents. Model fit was achieved using *P*-value, Fisher'C statistic and the Akaike information criterion corrected for small sample size (AICc). All analyses were conducted in R version 4.4.1.

3 | RESULTS

3.1 | Lignin phenol and amino sugar accumulations and their contributions to SOC under N addition

In the topsoil, total lignin phenol contents were notably higher in N-fertilized soils, with significant increases observed under $N_{2.30}$, $N_{4.60}$ and $N_{13.80}$ treatments. In contrast, subsoil lignin phenol contents showed a hump-shaped response to N inputs, peaking at $N_{4.60}$ ($p < 0.05$; Figure S3b). Across all N addition treatments, the lignin phenol pool was consistently dominated by V-type phenols, followed by S- and C- type phenols, in both soil layers (Figure S4a,c). High levels of N addition significantly raised the proportion of lignin phenols in topsoil SOC, whereas in the subsoil this proportion increased at low levels of N addition and subsequently declined, reaching a maximum at $N_{4.60}$ ($p < 0.05$; Figure 1A). Similarly, constituent proportions of lignin phenols in SOC tended to increase across the N gradient in the topsoil, but showed a hump-shaped response in the subsoil, peaking at intermediate N addition rates ($p < 0.05$; Figure 1B–D). The proportions of total lignin phenols and its constituents in SOC were significantly higher in topsoil than subsoil (all $p < 0.05$; Figure 1). The syringyl to vanillyl (S/V) and cinnamyl to vanillyl (C/V) ratios showed a trend of first increasing and then decreasing with increasing N addition in the topsoil, while in the subsoil both indices declined significantly (Figure 1E,F). N addition only significantly affected the subsoil ratio of acid to aldehyde units for both syringyl $(Ac/Al)_S$ and vanillyl $(Ac/Al)_V$, with both exhibiting negative hump-shaped responses ($p < 0.05$; Figure 1G,H).

Amino sugar contents were consistently higher in N-fertilized soils compared to controls in both topsoil and subsoil (Figure S3c), primarily due to increases in glucosamine and galactosamine contents (Figure S4b,d). With increasing N addition, the proportions of amino sugars, fungal-derived glucosamine and muramic acid in SOC were significantly increased in the topsoil, though they tended to decrease at high levels of N addition (all $p < 0.05$; Figure 2A–C). In contrast, in the subsoil, the proportions of amino sugars and fungal glucosamine exhibited significant increases only under $N_{1.15}$ and $N_{4.60}$ treatments, respectively, whereas the proportion of muramic acid in SOC significantly declined as N addition increased (all $p < 0.05$; Figure 2A–C). Across all treatments, amino sugars, fungal glucosamine and muramic acid contributed more to SOC in topsoil than in subsoil (all $p < 0.05$; Figure 2A–D). Notably, the ratios of fungal to bacterial amino sugar in response to N addition did not vary significantly in the topsoil but were significantly increased in the subsoil (Figure 2E,F).

3.2 | Responses of soil microbial community composition and K-/r-traits to N addition

Soil microbial community diversity and structure were significantly altered by N addition. Specifically, fungal Shannon diversity declined

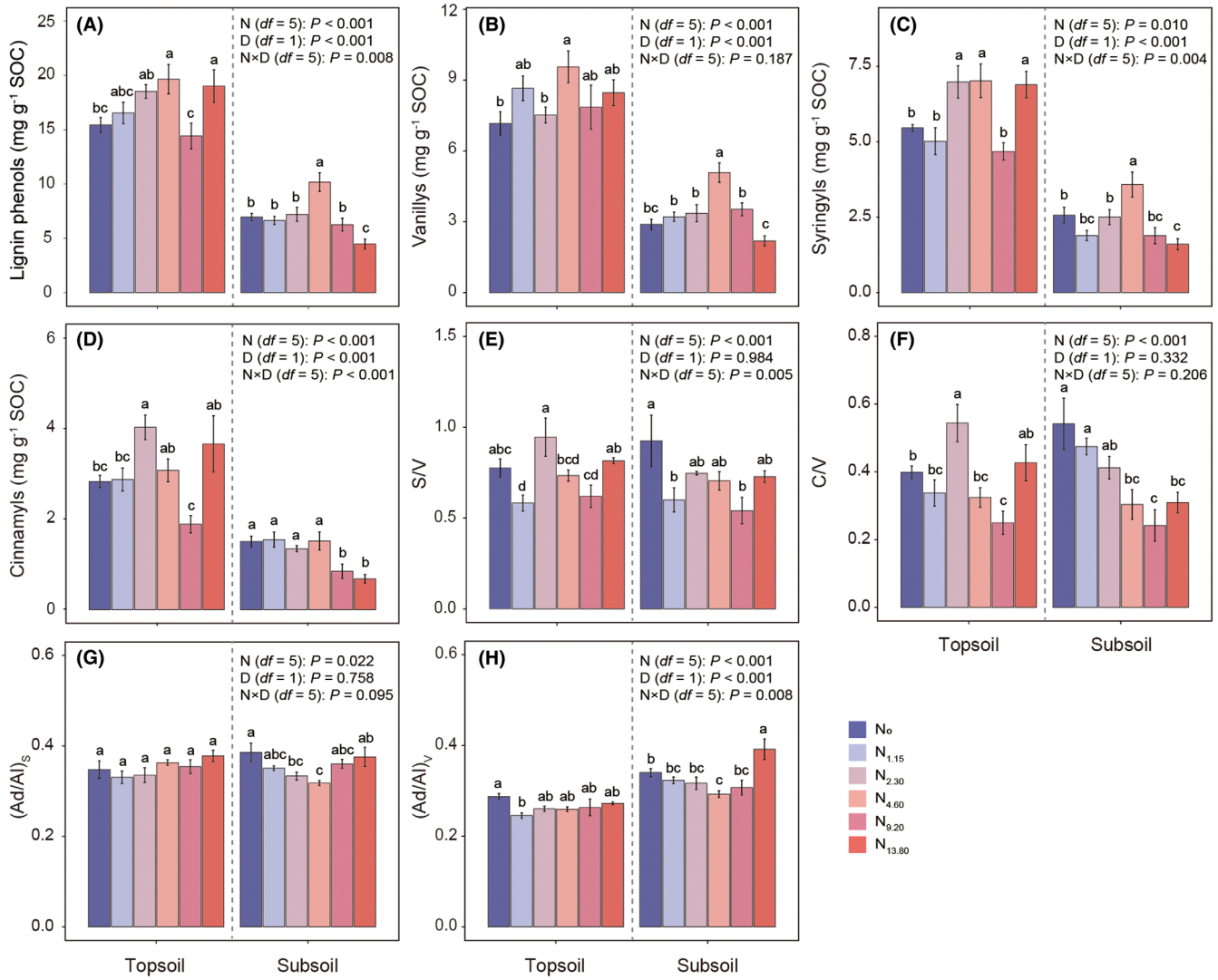

FIGURE 1 Effects of N addition on (A) the proportions of total lignin phenols in SOC, (B–D) the proportions of individual lignin phenols in SOC, (E) the ratios of syringyl to vanillyl (S/V), (F) the ratios of cinnamyl to vanillyl (C/V), (G) the acid to aldehyde ratios of syringyl units $(Ac/Al)_S$ and (H) the acid to aldehyde ratios of vanillyl units $(Ac/Al)_V$ in the topsoil and subsoil. Error bars represent the mean value (±SE) for each treatment ($n = 5$). Different lowercase letters above the error bars indicate significant differences among N addition treatments, as determined by *Duncan's* post hoc test at $p < 0.05$. N, N addition; D, soil depth; N × D, interaction of N addition and soil depth.

with N inputs in both topsoil and subsoil, whereas bacterial diversity was significantly enhanced only in the subsoil (Tables S8 and S9). Both fungal and bacterial taxonomic composition were clearly separated by N addition treatments across soil layers (both PERMANOVA $p < 0.05$; Figure 3, Figures S5 and S6). Network analyses showed that the relationships between fungal and bacterial taxa tended to be co-occurrences, with the dominant taxa being positively correlated in environments with N addition in both depths (Figure 3c,d,g,h). The fungal and bacterial taxa were grouped into four (Module#1–4) and three (Module#1–3) key ecological clusters in the topsoil and subsoil, respectively. In the topsoil, the abundances of taxa associated with Module#1 and Module#2 displayed hump-shaped responses to N addition, peaking at $N_{4.60}$, while in the subsoil, module abundances increased consistently with N input (all $p < 0.05$; Table S1, Figure S1). The higher modularity and node connectedness observed in topsoil indicated greater complexity of microbial networks relative to subsoil (Figure 3c,g).

To evaluate shifts in trophic strategies in response to N addition, the relative abundance of potential oligotrophic and copiotrophic fungal and bacterial taxa were summed (Table S2). Across all N treatments, copiotrophic (*r*-strategist) taxa remained dominant over oligotrophic (*K*-strategist) taxa for both bacteria and fungi in the topsoil and subsoil (Figures S5 and S6). The ratios of oligotrophs to copiotrophs associated with fungal taxa declined toward medium N application levels (i.e. $N_{9.20}$), then tended to increase at higher levels of N addition in both soil layers (both $p < 0.05$; Table S10, Figure 4a). In contrast, for bacterial taxa in the topsoil, the oligotrophs/copiotrophs ratios exhibited a significant negative hump-shaped response along the N addition gradients ($p < 0.05$; Table S10, Figure 4b). Additionally, abundances of functional genes

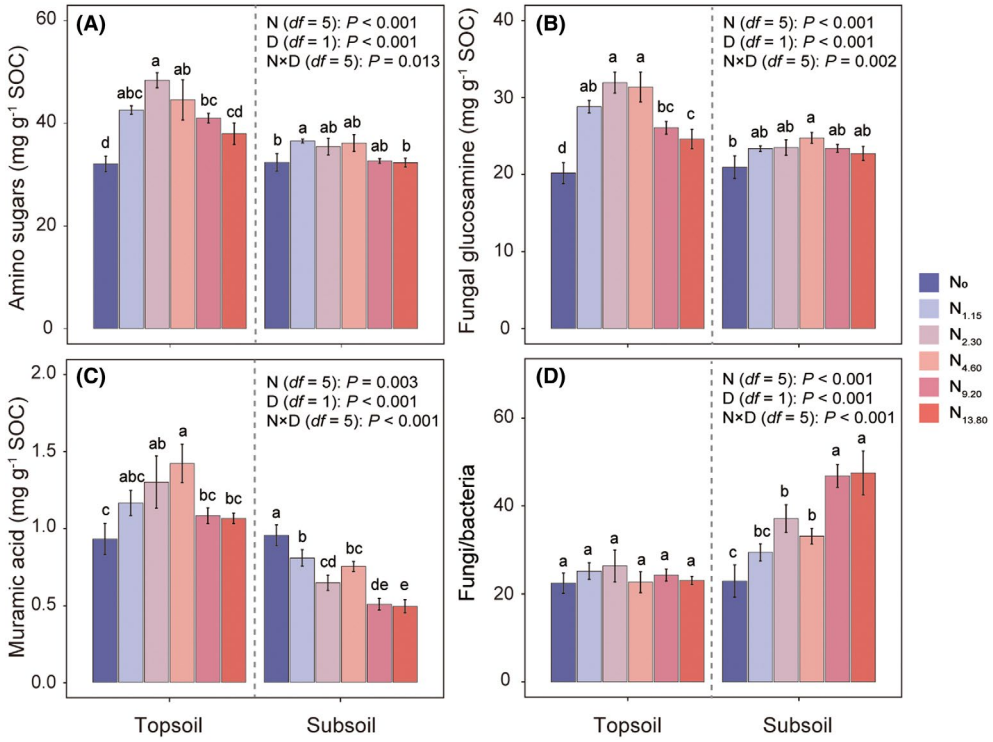

FIGURE 2 Effects of N addition on (A) the proportions of amino sugars in SOC, (B) the proportions of fungal glucosamine in SOC, (C) the proportions of muramic acid in SOC and (D) the ratios of fungal to bacterial biomarkers in the topsoil and subsoil. Error bars represent the mean value (±SE) for each treatment ($n = 5$). Different lowercase letters above the error bars indicate significant differences among N addition treatments, as determined by *Duncan's* post hoc test at $p < 0.05$. N, N addition; D, soil depth; N × D, interaction of N addition and soil depth.

involved in recalcitrant C turnover (oxidation of lignin, chitin and aromatics) and labile C turnover (hydrolysis of cellulose, hemicellulose and starch) were summed to assess potential life-history traits at the gene level (Table S10, Figure S2). Although the ratio of recalcitrant to labile C degradation genes (R/L genes) was unaffected by N addition in both soil layers, R/L gene ratios were consistently higher in topsoil than subsoil ($p < 0.05$; Figure 4c).

3.3 | Key drivers of lignin phenol and amino sugar accumulations under N addition

To identify the key drivers of lignin phenol and amino sugar accumulation in the two soil layers, we analysed the potential influence of different factors (i.e. plant properties, edaphic condition, mineral protection, microbial community composition and microbial *K*-/*r*-traits). In the topsoil, lignin phenols were positively correlated with PCI, DIN, $Fe_o + Al_o$, BG, NAG + LAP and Bacterial_PCoA1, but negatively correlated with clay + silt, Fungal_O/C and Bacterial_O/C (all $p < 0.05$; Figure 5a). In the subsoil, lignin phenols showed positive associations with Ca_{exe} and $Fe_o + Al_o$ and negative associations with Fungal_PCoA1 (all $p < 0.05$; Figure 5b). Similarly, amino sugars were also closely correlated with multiple factors, varying by soil layers: in the topsoil, amino sugars significantly increased with DOC, Ca_{exe}, $Fe_o + Al_o$, BG, NAG + LAP, Fungal_PCoA1 and the relative abundance of Module#1, but significantly decreased with clay + silt and Fungal_O/C (all $p < 0.05$; Figure 6a). In comparison, amino sugars in the subsoil were positively associated with PCI, Ca_{exe} and $Fe_o + Al_o$, but negatively associated with Fungal_O/C (all $p < 0.05$; Figure 6b). Boosted regression tree (BRT) analysis revealed that mineral protection and microbial features including microbial metabolism, microbial community composition and microbial *K*-/*r*-traits–played important roles in regulating lignin phenols and amino sugars in both the topsoil and subsoil (Figures 5h,i and 6h,i).

3.4 | Regulatory pathway of N addition on lignin phenol and amino sugar accumulations in topsoil and subsoil

To further elucidate the regulatory pathway of N addition on lignin phenols and amino sugars at two soil depths, SEM was performed. For the topsoil, lignin phenol and amino sugar accumulation were predominantly and directly regulated by microbial *K*-/*r*-traits and microbial community composition, respectively, with a standardized direct effect of 0.51 and 0.38(Figure 7a,b). Plant C input and mineral protection exerted indirect effects on lignin phenols by

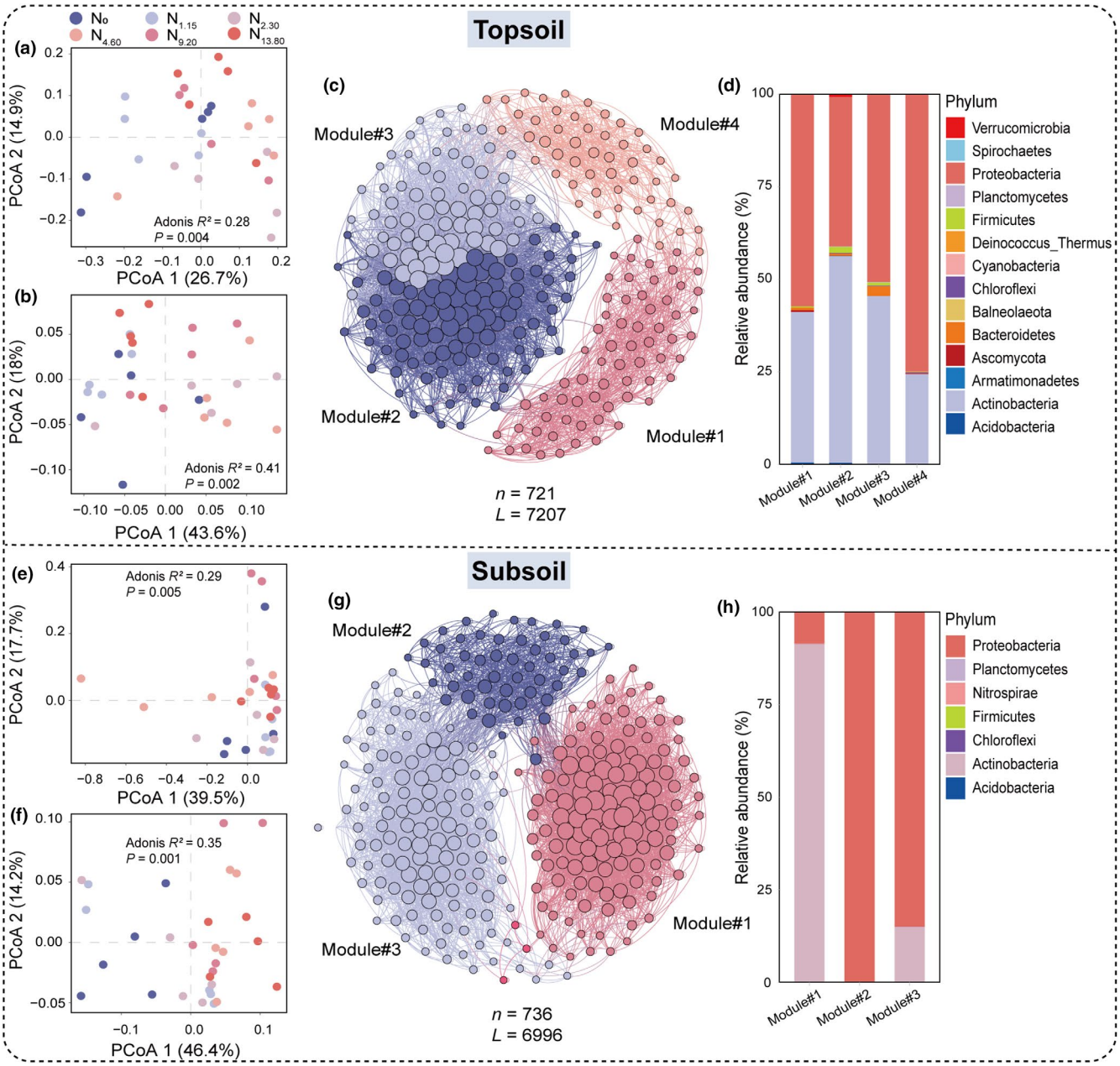

FIGURE 3 Effects of N addition on soil microbial community diversity and the main ecological clusters of co-occurrence networks in the topsoil and subsoil. Compositional similarity of microbial communities (β-diversity) is represented as PCoA ordination plots for fungi (a, e) and bacteria (b, f), estimated using Weighted Unifrac distance matrices. Network diagram with nodes (OTUs) coloured according to the main ecological clusters in the topsoil (Modules#1–4, c) and subsoil (Modules#1–3, g). Details of network topological attributes for each main ecological cluster are listed in Table S3. Relative abundances of the dominant species in each main ecological cluster are shown for the topsoil (d) and subsoil (h).

regulating microbial *K*-/r-traits, while DOC indirectly regulated amino sugars via microbial community composition (Figure 7a,b). By contrast, subsoil lignin phenols were significantly and directly regulated by microbial community composition and mineral protection, with standardized direct effects of 0.47 and 0.48, respectively (Figure 7c). Subsoil amino sugars were significantly and directly modulated by plant C input, mineral protection and microbial *K*-/r-traits, collectively explaining 52% of the total variation in amino sugars (Figure 7d).

4 | DISCUSSION

4.1 | Effects of N addition on the accumulation of plant lignin phenols and microbial residues, and their contribution to SOC formation

Our study demonstrates that long-term N addition enhances lignin phenol accumulation and its contribution to SOC in the topsoil; however, this effect plateaus once a certain threshold is reached

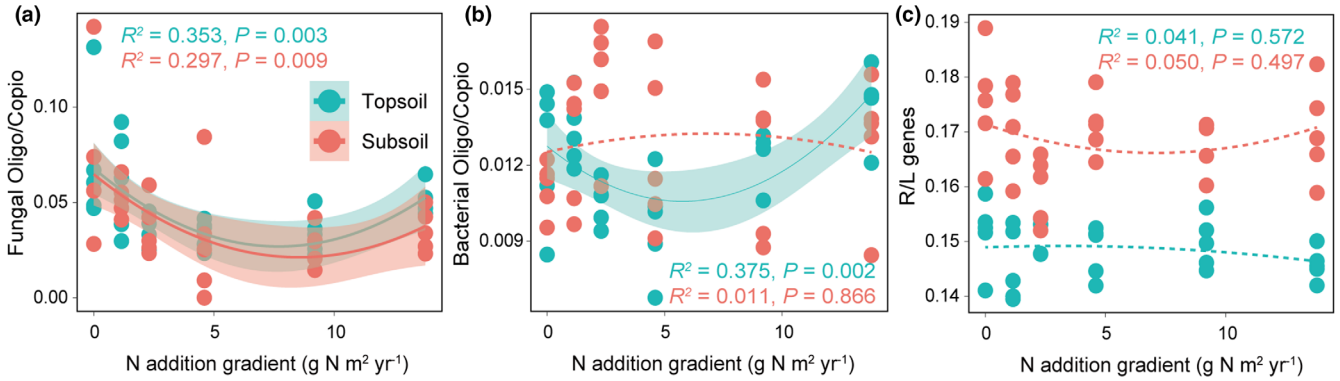

FIGURE 4 Microbial *K*-/*r*-strategy ratios in response to increasing N addition in the topsoil and subsoil: (a) Fungal oligotroph/copiotroph ratio; (b) Bacterial oligotroph/copiotroph ratio; (c) Recalcitrant/labile organic carbon degradation gene abundance ratio (R/L genes). Fitted lines depict quadratic functions with 95% confidence intervals (shaded section).

(Figure 1a and Figure S3b). Under N-limited conditions, N inputs promote plant growth and litter accumulation, thereby increasing lignin inputs from shoots and roots (Ye et al., 2018). At higher N levels ($N_{4.60}$–$N_{13.80}$), however, although plant biomass continues to increase (Figure S7), microbial growth may shift to C limitation (Yuan, Niu, Gherardi, et al., 2019). In this case, microbes preferentially decompose more labile plant residues to meet their C demand, thereby offsetting the stimulating effect of increased plant biomass on lignin phenol formation and accumulation (He et al., 2024; Huang et al., 2023). In the subsoil, the response of lignin phenol accumulation to N addition was much smaller (*Hedges'g* = 0.00) than in the topsoil (*Hedges'g* = 0.73), likely due to lower plant C input (Figure S7), fewer resistant phenols (Kiem & Kögel-Knabner, 2003) and increased microbial oxidation under C-limited conditions (Kösters et al., 2018; Li et al., 2023). Elevated (Ac/Al)s and (Ac/Al)v ratios under high N further support increased oxidative breakdown (Figure 1 and Figure S8).

In line with the microbial C pump (Feng & Wang, 2023; Liang et al., 2017), N addition also promoted amino sugar accumulation and their contribution to SOC in both soil layers (Figure 2a and Figure S3c), while again this effect declined under excessive N fertilization. Moderate N inputs likely enhanced microbial growth via increased plant-derived C, while high N levels led to acidification and Al^{3+} toxicity, suppressing microbial activity (Xing et al., 2022; Ye et al., 2018). Fungal residues contributed more to SOC than bacterial residues across depths (Figure 2), consistent with prior studies (Hu, Deng, et al., 2024; Luo et al., 2021; Ma, Ju, et al., 2022). This dominance likely stems from fungi's tolerance to low pH (Rousk et al., 2010), their enzymatic ability to degrade complex plant polymers (Angst et al., 2021; Sokol et al., 2022) and more efficient mineral protection of fungal cell wall fragments (Luo et al., 2021; Zou et al., 2023).

Importantly, the increase in amino sugar exceeded the increase in lignin phenols, especially in the subsoil (Figure 1 and Figure S9), supporting our hypothesis that microbial residues are the dominant contributors to SOC under N enrichment. While some agricultural and forest studies report greater plant-derived SOC increases (Takele et al., 2025; Zou et al., 2023), our findings reinforce the view that SOC formation is shaped by the balance between plant inputs and microbial transformation (Lavallee et al., 2020; Schmidt et al., 2011). Although N addition boosted plant C inputs (Figure S7), it also altered microbial communities and stimulated microbial growth (Figure 3, Figures S5, S6 and S10). Under low levels of N addition, microbes may degrade recalcitrant lignin to meet nutrient demands, limiting lignin accumulation. With increased N inputs, microbial limitation shifted from N to C. This drives microbes to produce C-acquiring enzymes and co-metabolize lignin phenols, accelerating their decomposition (Bahri et al., 2008; Li et al., 2023). In contrast, alleviation of N limitation reduces the need for energy-costly N-acquiring enzymes (Allison & Vitousek, 2005), slowing microbial residue turnover and promoting their preservation. Furthermore, N enrichment enhances fungal residue formation, which is structurally more resistant to decomposition than bacterial residues (Angst et al., 2021; He et al., 2022; Ma et al., 2018). Collectively, these findings highlight that microbial residues—especially from fungi—play a more pivotal role than plant-derived lignin phenols in SOC accumulation under elevated N deposition in grasslands.

4.2 | Key drivers regulating the accumulation of plant-derived lignin phenols and microbial residues under N addition

Our results showed that the accumulation of plant-derived lignin phenols in topsoil was primarily regulated by fungal and bacterial *K*-/*r*-traits, while the accumulation of amino sugars was directly controlled by fungal community composition and the abundance of Module#1 under N additions (Figures 5–7). These findings indicate microbial traits are the key drivers of lignin phenol and amino sugar accumulation in topsoil, partially supporting our second hypothesis. Although previous research has highlighted the importance of microbial physiology and community structure in regulating lignin phenol accumulation (Angst et al., 2021; Huang et al., 2023; Ma et al., 2018; Whalen et al., 2022), studies at the phylogenetic level remain limited.

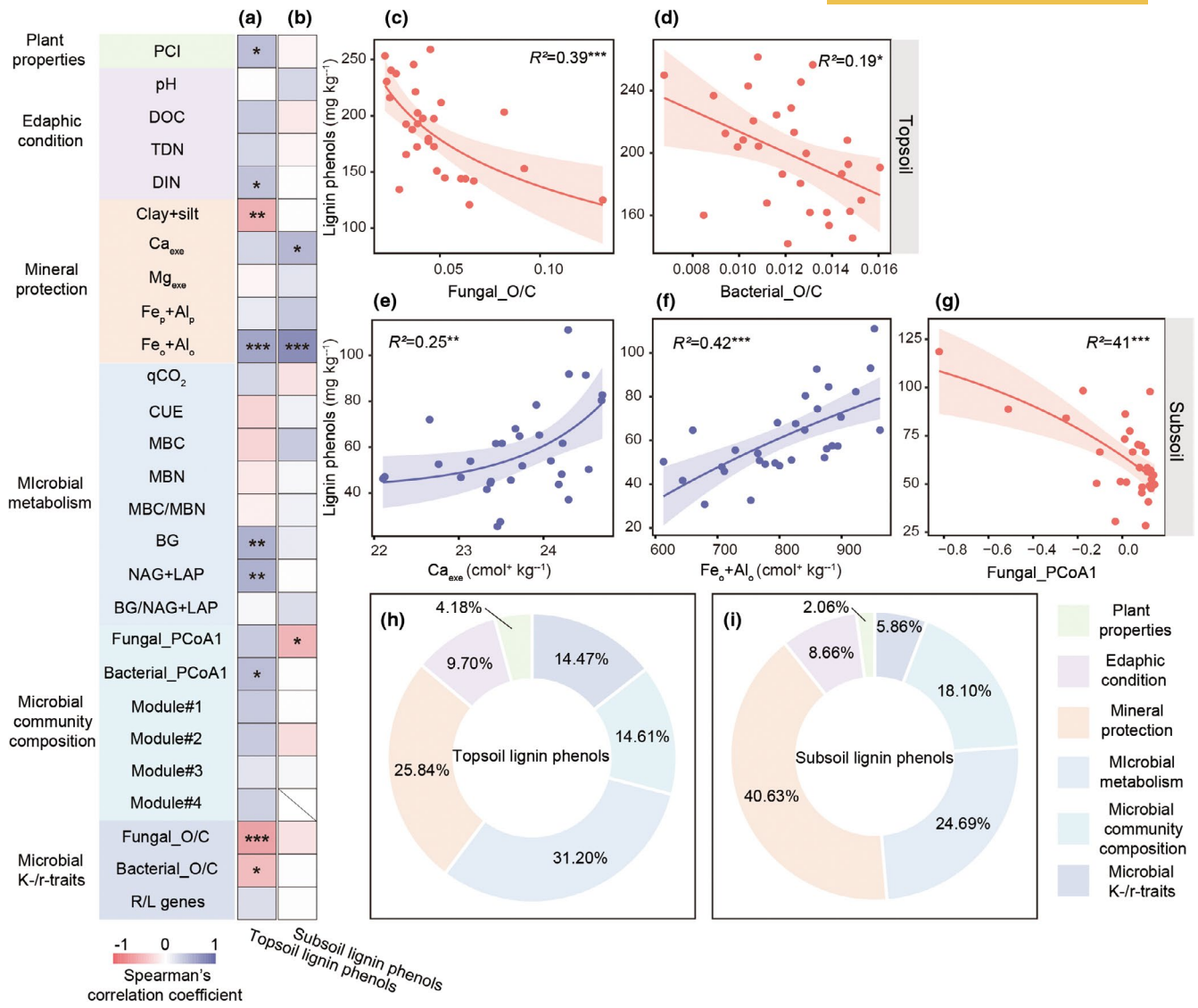

FIGURE 5 Relationships between lignin phenols and biotic and abiotic factors along an N addition gradient in topsoil and subsoil: (a, b) spearman correlations of biotic and abiotic factors with lignin phenols, (c–g) relationships of lignin phenols with mineral protection, microbial community composition and microbial *K*-/*r*-traits, and (h, i) boosted regression tree (BRT) analysis illustrating the relative contributions of plant properties, edaphic condition, mineral protection, microbial metabolism, microbial community composition and microbial *K*-/*r*-traits to lignin phenols. *, ** and *** indicate statistical significance at $p < 0.05$, $p < 0.01$ and $p < 0.001$, respectively. Abbreviations are defined as follows: PCI, plant carbon input; DOC, dissolved organic carbon; DIN, dissolved inorganic nitrogen; TDN, total dissolved nitrogen; Ca_{exe}, exchangeable Ca^{2+}; Mg_{exe}, exchangeable Mg^{2+}; $Fe_p + Al_p$, sum of pyrophosphate-extractable Fe/Al oxides; $Fe_o + Al_o$, sum of oxalate-extractable Fe/Al oxides; CUE, carbon use efficiency; MBC, microbial biomass carbon; MBN, microbial biomass nitrogen; BG, β-1,4-glucosidase activity; NAG + LAP, N-acetyl-β-D-glucosaminidase + leucine aminopeptidase activity; Fungal_PCoA1, the first dimensional PCoA ordination of taxonomic composition for fungal community; Bacterial_PCoA1, the first dimensional PCoA ordination of taxonomic composition for bacterial community; Fungal_O/C, fungal oligotroph/copiotroph ratio; Bacterial_O/C, bacterial oligotroph/copiotroph ratio; R/L genes, recalcitrant/labile organic carbon degradation gene abundance ratio.

In this study, we linked lignin phenols with microbial *K*-/*r*-strategist traits, defined by specific taxa and functional genes under N deposition. The direct regulation of plant lignin phenols by fungal and bacterial *K*-/*r*-traits suggests that changes caused by N addition can be explained by the microbial *K*/*r* selection theory. Previous work has demonstrated that oligotrophic (*K*-strategist) taxa efficiently decompose recalcitrant substrates, while copiotrophic (*r*-strategist) taxa display faster growth and a stronger capacity for utilizing labile substrates (Fierer et al., 2007; Li et al., 2021). Consequently, we proposed that a higher oligotroph-to-copiotroph ratio enhances lignin phenol decomposition—a hypothesis supported by the significant negative correlations observed between Fungal_O/C, Bacterial_O/C and lignin phenols (Figure 5 and Figure S11).

In contrast, the accumulation of amino sugars in topsoil was associated with fungal community composition and the abundance of Module#1 (Figure 6). This could be attributed to the high tolerance

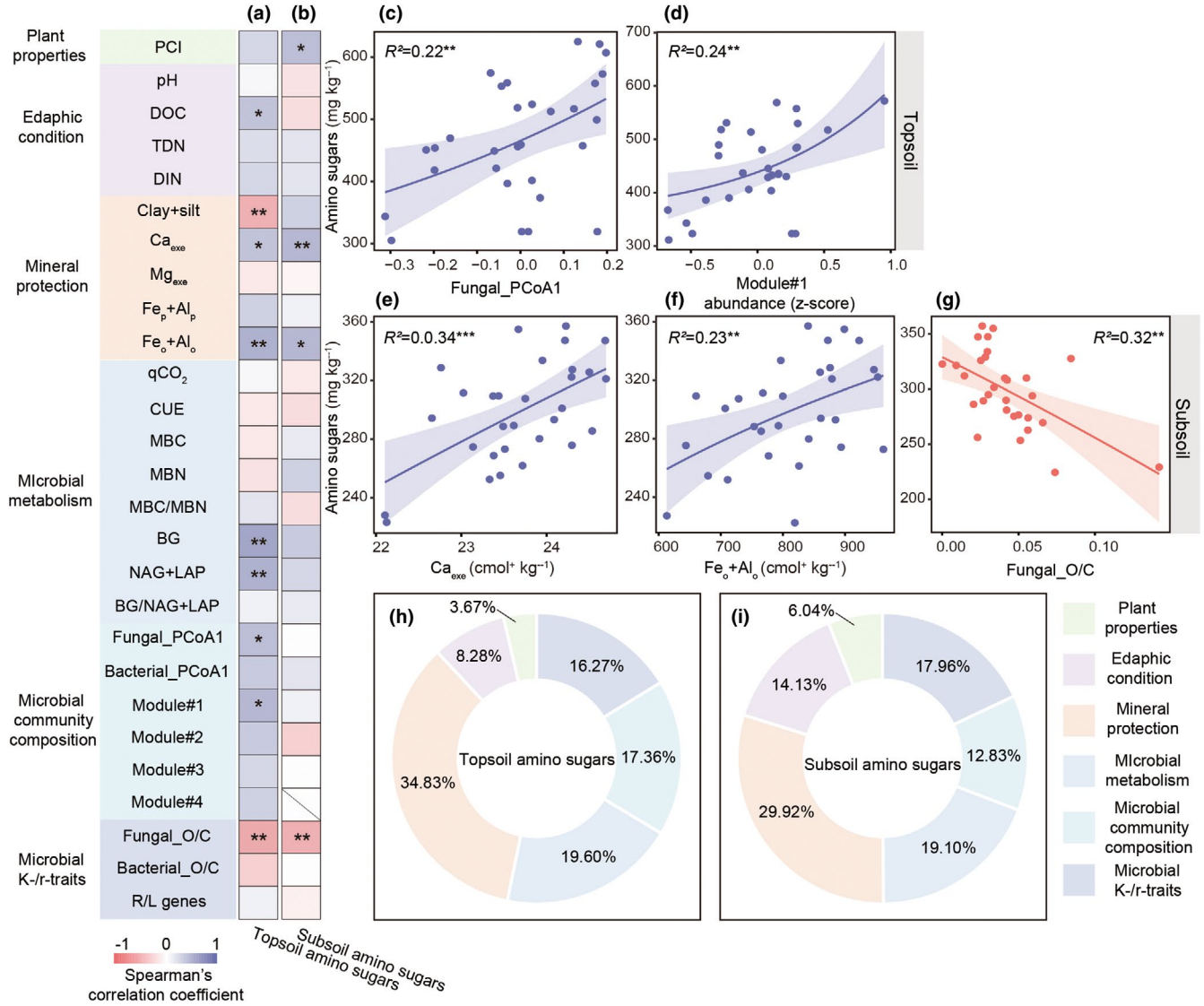

FIGURE 6 Relationships between amino sugars and biotic and abiotic factors along an N addition gradient in topsoil and subsoil: (a, b) spearman correlations of biotic and abiotic factors with amino sugars, (c–g) relationships of amino sugars with mineral protection, microbial community composition and microbial *K*-/*r*-traits, and (h, i) boosted regression tree (BRT) analysis illustrating the relative contributions of plant properties, edaphic condition, mineral protection, microbial metabolism, microbial community composition and microbial *K*-/*r*-traits to amino sugars. *, ** and *** indicate statistical significance at $p < 0.05$, $p < 0.01$ and $p < 0.001$, respectively. See Figure 6 for abbreviations.

of fungi to environmental disturbances (Kaiser et al., 2014; Li et al., 2021) and the high efficiency and stability of their residue (Luo et al., 2021; Zou et al., 2023), which together promote the formation and retention of microbial residues. Moreover, previous studies have reported that N addition can alter microbial co-occurrence networks, leading to the aggregation of species with similar environmental and resource needs into distinct ecological clusters, thereby influencing soil C and N sequestration and cycling (Fan et al., 2019; Jiao et al., 2022; Ma, Wang, et al., 2022; Zhang, Niu, et al., 2025). In line with these findings, we observed a positive correlation between Module#1 abundance and amino sugar accumulation (Figure 6), highlighting the role of microbial ecological clusters in maintaining microbial residue levels. This may be because Module#1 is dominated by Actinobacteria and Proteobacteria (Figure 3), both classified as r-strategists (Fierer et al., 2007), which efficiently utilize soil resources to maintain high metabolic and turnover demands (Craig et al., 2022; Kaiser et al., 2014; Wang et al., 2022), thereby promoting microbial residue production. Additionally, this study found that plant C inputs and DOC content indirectly promoted the accumulation of lignin phenols and amino sugars by influencing microbial traits (Figure 7a,b). This could be because increases in plant-derived C and DOC might trigger a priming effect by enhancing microbial activity, cell proliferation and turnover rates, contributing to the production of lignin phenols and amino sugars (Huang et al., 2023).

Under N additions, the accumulation of plant-derived lignin phenols and amino sugars in the subsoil was primarily driven by Ca_{exe}, Fe_o+Al_o, fungal community composition and Ca_{exe}, Fe_o+Al_o and fungal *K*-/*r*-traits, respectively (Figures 5–7). This finding indicates

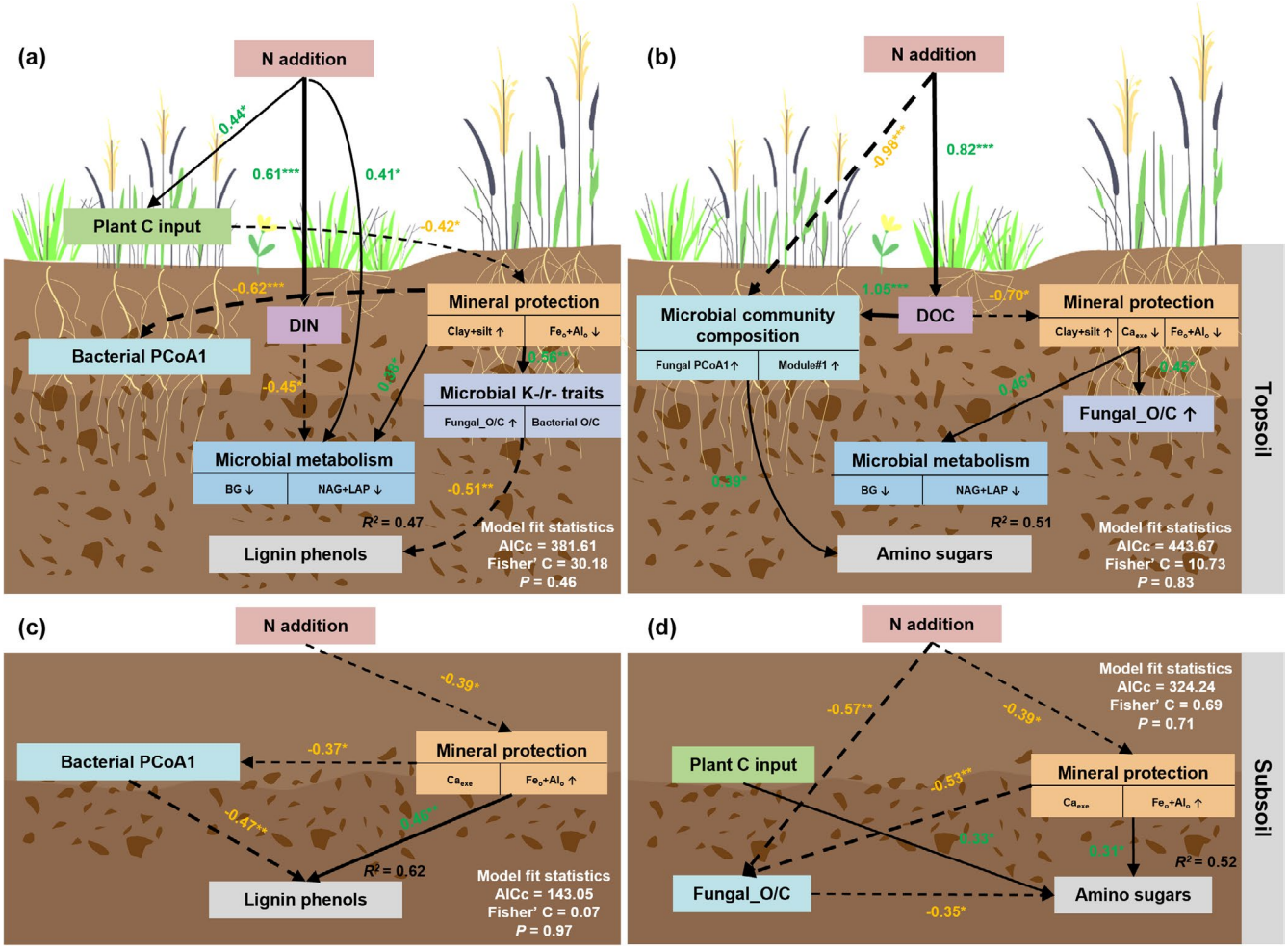

FIGURE 7 Structure equation modelling (SEM) analysis illustrating the multivariate effects on lignin phenols and amino sugars under N addition in the topsoil (a, b) and subsoil (c, d). Path coefficients (correlation coefficients) along the arrows are standardized by the mean of each parameter. Arrow widths correspond to the effect size. Black solid and dashed arrows indicate positive and negative relationships, respectively. The multiple-layer rectangles represent the PC1 from the principal components analysis (PCA) of mineral protection, microbial metabolism, microbial community composition and microbial *K*-/*r*-traits. Percentages adjacent to variables indicate the variance explained by the model (R^2). The symbols '↑' and '↓' beside the variables denote significant positive and negative relationships with the PC1 from the PCA, respectively. *, ** and *** indicate statistically significant at $p < 0.05$, $p < 0.01$ and $p < 0.001$, respectively. See Figure 6 for abbreviations.

that both microbial traits and mineral protection are key factors in predicting the buildup of these compounds in the subsoil. Compared to the topsoil, the subsoil's lower nutrient availability as well as sub-optimal conditions, such as oxygen deficiency, favour fungal growth and reproduction. Consequently, shifts in fungal community composition and competitive interactions with other microbial taxa may either suppress or enhance the decomposition of lignin phenols and amino sugars (He et al., 2022; Huang et al., 2023; Liu et al., 2023). This is supported by the significant negative correlations between lignin phenols and fungal community composition (Fungal_PCoA1), and between amino sugars and Fungal_O/C in the subsoil (Figures 5g and 6g). We note, however, that shotgun metagenomics may underestimate certain fungal groups, particularly Glomeromycota (arbuscular mycorrhizal fungi), due to their underrepresentation in reference databases (Tedersoo et al., 2022), which should be taken into account when interpreting fungal community responses.

Indeed, previous studies have shown that the physical and chemical protection provided by soil minerals plays a stronger role in maintaining the long-term stability of lignin phenols and amino sugars in the subsoil compared to the topsoil (He et al., 2022). For example, the larger specific surface area of soil silt and clay particles could promote the formation of microaggregates, which would physically occlude lignin phenols, preventing their decomposition and utilization (Angst et al., 2021; Ma et al., 2018; Wang et al., 2022). Additionally, soil exchangeable cations (e.g. Ca_{exe}) could form inner- and outer-sphere bridges with functional groups on amino sugars, facilitating the adsorption and stabilization of microbial residues (He et al., 2022; Hu et al., 2022; Rowley et al., 2018). Furthermore, Fe/Al oxides could promote the transformation of amino sugars into more stable MAOC through ligand exchange or co-precipitation (Kallenbach et al., 2016; Whalen et al., 2022). Consistent with these findings, our study observed significant positive correlations

between lignin phenols, amino sugars and both Ca_{exe} and $Fe_o + Al_o$ in subsoil (Figures 5b,e,f and 6b,e,f), suggesting that enhanced mineral protection induced by N addition promoted the formation of organic-mineral complexes, thereby stabilizing lignin phenols and amino sugars (Figure 7). Additionally, BRT analysis revealed that the relative importance of mineral protection in regulating the accumulation of lignin phenols and amino sugars was greater in the subsoil than in the topsoil (Figures 5h,i and 6h,i), further supporting this deduction. Overall, these findings emphasize that under long-term N addition, the accumulation of plant-derived lignin phenols and microbial residues in topsoil is primarily controlled by microbial traits, whereas in the subsoil, both microbial traits and mineral protection jointly regulate their accumulation. We acknowledge that the relationships reported here are correlative and do not demonstrate causality per se; thus, the mechanistic interpretations above should be regarded as working hypotheses that require further testing with targeted experiments.

5 | CONCLUSIONS

Understanding how long-term N addition affects plant-derived lignin phenols, microbial residues and their controls is key to predicting soil carbon sequestration under global change. This study showed that microbial residues, particularly those derived from fungi, disproportionately contributed to SOC accumulation under elevated N, accounting for 52%–67% of SOC increases, compared to only 23%–31% from plant-derived lignin phenols. These findings challenge the traditional plant-centric models of SOC formation and highlight the necessity of explicitly incorporating microbial C pumps into Earth System Models. We also detected that factors controlling their accumulation varied by depth, with microbial community traits dominating in topsoil and combined microbial–mineral interactions prevailing in subsoil, indicating that single-layer soil C models may misrepresent SOC dynamics. Therefore, Earth System Models should incorporate such depth-dependent processes for more accurate SOC predictions under future global change scenarios. While plant- and microbial-derived residues are known to mainly form particulate or mineral-associated organic C, it is unclear how the addition of N changes this distribution. We recommend long-term ^{13}C isotope tracing using labelled litter or rhizodeposits to elucidate the respective contributions of plant- and microbial-derived C into particulate and mineral-associated SOC fractions.

AUTHOR CONTRIBUTIONS

Xiaobo Yuan, Guiyao Zhou and Zengru Wang conceived the ideas and designed methodology; Xiaobo Yuan, Shize Yao, Ying Wang, Tian Ma, Ning Chen, Yaodan Zhang, Jingrun Xu, Shujuan Wu, Mengfei Zhang, Yaodong Li, Baoming Du, Peijing Chang and Tianhu Han collected the data; Xiaobo Yuan, Shize Yao, Yaodan Zhang, Jingrun Xu, Decao Niu, Hua Fu and Zengru Wang analysed the data; Xiaobo Yuan, Shize Yao, Guiyao Zhou, Adam Frew, Peter Dietrich, Yuan Li, Ying Wang and Zengru Wang led the writing of the manuscript. All authors contributed critically to the drafts and gave final approval for publication.

ACKNOWLEDGEMENTS

This work was sponsored by the National Key Research and Development Program of China (2023YFF0806800), National Natural Science Foundation of China (32101445), Natural Science Foundation of Gansu Province of China (22JR5RA467) and the Initial Funding of Scientific Research for Imported Talents of Lanzhou University (561121201), Alxa League Science and Technology Program (AMYY2022-16). The authors are grateful to the Semi-Arid Climate and Environment Observatory of Lanzhou University (SACOL) for supporting the fieldwork.

CONFLICT OF INTEREST STATEMENT

The authors declare that they have no conflict of interest.

DATA AVAILABILITY STATEMENT

Data upon which this study is based are available through the Dryad Digital Repository: https://doi.org/10.5061/dryad.866t1g25j (Yuan, 2026).

ORCID

Xiaobo Yuan https://orcid.org/0009-0001-4834-238X
Guiyao Zhou https://orcid.org/0000-0002-1385-3913
Adam Frew https://orcid.org/0000-0001-9859-2419
Yuan Li https://orcid.org/0000-0003-1047-0690
Ning Chen https://orcid.org/0000-0002-1779-915X
Baoming Du https://orcid.org/0000-0002-1020-0642
Decao Niu https://orcid.org/0000-0003-2607-043X
Hua Fu https://orcid.org/0000-0003-1526-9304

REFERENCES

Allison, S. D., & Vitousek, P. M. (2005). Responses of extracellular enzymes to simple and complex nutrient inputs. *Soil Biology and Biochemistry*, *37*, 937–944. https://doi.org/10.1016/j.soilbio.2004.09.014

Angst, G., Mueller, K. E., Nierop, K. G. J., & Simpson, M. J. (2021). Plant- or microbial-derived? A review on the molecular composition of stabilized soil organic matter. *Soil Biology and Biochemistry*, *156*, 108189. https://doi.org/10.1016/j.soilbio.2021.108189

Angst, Š., Angst, G., Mueller, K. E., Lange, M., & Eisenhauer, N. (2025). Un(der)explored links between plant diversity and particulate and mineral-associated organic matter in soil. *Nature Communications*, *16*, 5548. https://doi.org/10.1038/s41467-025-60712-6

Bahri, H., Rasse, D. P., Rumpel, C., Dignac, M. F., Bardoux, G., & Mariotti, A. (2008). Lignin degradation during a laboratory incubation followed by ^{13}C isotope analysis. *Soil Biology and Biochemistry*, *40*, 1916–1922. https://doi.org/10.1016/j.soilbio.2008.04.002

Balesdent, J., Basile-Doelsch, I., Chadoeuf, J., Cornu, S., Derrien, D., Fekiacova, Z., & Hatté, C. (2018). Atmosphere-soil carbon transfer as a function of soil depth. *Nature*, *559*, 599–602. https://doi.org/10.1038/s41586-018-0328-3

Carson, C. M., & Zeglin, L. H. (2018). Long-term fire management history affects N-fertilization sensitivity, but not seasonality, of grassland soil microbial communities. *Soil Biology and Biochemistry*, *121*, 231–239. https://doi.org/10.1016/j.soilbio.2018.03.023

Carvalhais, N., Forkel, M., Khomik, M., Bellarby, J., Jung, M., Migliavacca, M., Mu, M., Saatchi, S., Santoro, M., Thurner, M., Weber, U., Ahrens, B., Beer, C., Cescatti, A., Randerson, J. T., & Reichstein, M. (2014). Global covariation of carbon turnover times with climate in terrestrial ecosystems. *Nature*, *514*, 213–217. https://doi.org/10.1038/nature13731

Chen, L., Liu, L., Mao, C., Qin, S., Wang, J., Liu, F., Blagodatsky, S., Yang, G., Zhang, Q., Zhang, D., Yu, J., & Yang, Y. (2018). Nitrogen availability regulates topsoil carbon dynamics after permafrost thaw by altering microbial metabolic efficiency. *Nature Communications*, *9*, 3951. https://doi.org/10.1038/s41467-018-06232-y

Chen, S., Chen, B., Wang, S., Sun, L., Shi, H., Liu, Z., Wang, Q., Li, H., Zhu, T., Li, D., Xia, Y., Zhao, Z., Wang, L., & Wang, L. (2023). Spatiotemporal variations of atmospheric nitrogen deposition in China during 2008-2020. *Atmospheric Environment*, *315*, 120120. https://doi.org/10.1016/j.atmosenv.2023.120120

Chen, X., Hu, Y., Xia, Y., Zheng, S., Ma, C., Rui, Y., He, H., Huang, D., Zhang, Z., Ge, T., Wu, J., Guggenberger, G., Kuzyakov, Y., & Su, Y. (2021). Contrasting pathways of carbon sequestration in paddy and upland soils. *Global Change Biology*, *27*, 2478–2490. https://doi.org/10.1111/gcb.15595

Christiansen, C. T., Engel, K., Hall, M., Neufeld, J. D., Walker, V. K., & Grogan, P. (2025). Arctic tundra soil depth, more than seasonality, determines active layer bacterial community variation down to the permafrost transition. *Soil Biology and Biochemistry*, *200*, 109624. https://doi.org/10.1016/j.soilbio.2024.109624

Cotrufo, M. F., Haddix, M. L., Kroeger, M. E., & Stewart, C. E. (2022). The role of plant input physical-chemical properties, and microbial and soil chemical diversity on the formation of particulate and mineral-associated organic matter. *Soil Biology and Biochemistry*, *168*, 108648. https://doi.org/10.1016/j.soilbio.2022.108648

Cotrufo, M. F., Wallenstein, M. D., Boot, C. M., Denef, K., & Paul, E. (2013). The microbial efficiency-matrix stabilization (MEMS) framework integrates plant litter decomposition with soil organic matter stabilization: Do labile plant inputs form stable soil organic matter? *Global Change Biology*, *19*, 988–995. https://doi.org/10.1111/gcb.12113

Craig, M. E., Geyer, K. M., Beidler, K. V., Brzostek, E. R., Frey, S. D., Stuart Grandy, A., Liang, C., & Phillips, R. P. (2022). Fast-decaying plant litter enhances soil carbon in temperate forests but not through microbial physiological traits. *Nature Communications*, *13*, 1229. https://doi.org/10.1038/s41467-022-28715-9

Crowther, T. W., Riggs, C., Lind, E. M., Borer, E. T., Seabloom, E. W., Hobbie, S. E., Wubs, J., Adler, P. B., Firn, J., Gherardi, L., Hagenah, N., Hofmockel, K. S., Knops, J. M. H., McCulley, R. L., MacDougall, A. S., Peri, P. L., Prober, S. M., Stevens, C. J., & Routh, D. (2019). Sensitivity of global soil carbon stocks to combined nutrient enrichment. *Ecology Letters*, *22*, 936–945. https://doi.org/10.1111/ele.13258

Crowther, T. W., van den Hoogen, J., Wan, J., Mayes, M. A., Keiser, A. D., Mo, L., Averill, C., & Maynard, D. S. (2019). The global soil community and its influence on biogeochemistry. *Science*, *365*, eaav0550. https://doi.org/10.1126/science.aav0550

Csardi, M. G. (2013). Package 'igraph'.

DeForest, J. L. (2009). The influence of time, storage temperature, and substrate age on potential soil enzyme activity in acidic forest soils using MUB-linked substrates and L-DOPA. *Soil Biology and Biochemistry*, *41*, 1180–1186. https://doi.org/10.1016/j.soilbio.2009.02.029

Domeignoz-Horta, L. A., Cappelli, S. L., Shrestha, R., Gerin, S., Lohila, A. K., Heinonsalo, J., Nelson, D. B., Kahmen, A., Duan, P., Sebag, D., Verrecchia, E., & Laine, A.-L. (2024). Plant diversity drives positive microbial associations in the rhizosphere enhancing carbon use efficiency in agricultural soils. *Nature Communications*, *15*, 8065. https://doi.org/10.1038/s41467-024-52449-5

Fan, K., Delgado-Baquerizo, M., Guo, X., Wang, D., Wu, Y., Zhu, M., Yu, W., Yao, H., Zhu, Y., & Chu, H. (2019). Suppressed N fixation and diazotrophs after four decades of fertilization. *Microbiome*, *7*, 143. https://doi.org/10.1186/s40168-019-0757-8

Feng, X., & Wang, S. (2023). Plant influences on soil microbial carbon pump efficiency. *Global Change Biology*, *29*, 3854–3856. https://doi.org/10.1111/gcb.16728

Fierer, N., Bradford, M. A., & Jackson, R. B. (2007). Toward an ecological classification of soil bacteria. *Ecology*, *88*, 1354–1364. https://doi.org/10.1890/05-1839

Galloway, J. N., Townsend, A. R., Erisman, J. W., Bekunda, M., Cai, Z., Freney, J. R., Martinelli, L. A., Seitzinger, S. P., & Sutton, M. A. (2008). Transformation of the nitrogen cycle: Recent trends, questions, and potential solutions. *Science*, *320*, 889–892. https://doi.org/10.1126/science.1136674

Gentsch, N., Wild, B., Mikutta, R., Čapek, P., Diáková, K., Schrumpf, M., Turner, S., Minnich, C., Schaarschmidt, F., Shibistova, O., Schnecker, J., Urich, T., Gittel, A., Šantrůčková, H., Bárta, J., Lashchinskiy, N., Fuß, R., Richter, A., & Guggenberger, G. (2018). Temperature response of permafrost soil carbon is attenuated by mineral protection. *Global Change Biology*, *24*, 3401–3415. https://doi.org/10.1111/gcb.14316

Gruba, P., & Mulder, J. (2015). Tree species affect cation exchange capacity (CEC) and cation binding properties of organic matter in acid forest soils. *Science of the Total Environment*, *511*, 655–662. https://doi.org/10.1016/j.scitotenv.2015.01.013

Guseva, K., Darcy, S., Simon, E., Alteio, L. V., Montesinos-Navarro, A., & Kaiser, C. (2022). From diversity to complexity: Microbial networks in soils. *Soil Biology and Biochemistry*, *169*, 108604. https://doi.org/10.1016/j.soilbio.2022.108604

He, J., Nie, Y., Tan, X., Hu, A., Li, Z., Dai, S., Ye, Q., Zhang, G., & Shen, W. (2024). Latitudinal patterns and drivers of plant lignin and microbial necromass accumulation in forest soils: Disentangling microbial and abiotic controls. *Soil Biology and Biochemistry*, *194*, 109438. https://doi.org/10.1016/j.soilbio.2024.109438

He, M., Fang, K., Chen, L., Feng, X., Qin, S., Kou, D., He, H., Liang, C., & Yang, Y. (2022). Depth-dependent drivers of soil microbial necromass carbon across Tibetan alpine grasslands. *Global Change Biology*, *28*, 936–949. https://doi.org/10.1111/gcb.15969

Hedges, J. I., & Ertel, J. R. (1982). Characterization of lignin by gas capillary chromatography of cupric oxide oxidation products. *Analytical Chemistry*, *54*, 174–178. https://doi.org/10.1021/ac00239a007

Hu, J., Huang, C., Zhou, S., Liu, X., & Dijkstra, F. A. (2022). Nitrogen addition increases microbial necromass in croplands and bacterial necromass in forests: A global meta-analysis. *Soil Biology and Biochemistry*, *165*, 108500. https://doi.org/10.1016/j.soilbio.2021.108500

Hu, Y., Deng, Q., Kätterer, T., Olesen, J. E., Ying, S., Ochoa-Hueso, R., Mueller, C. W., Weintraub, M. N., & Chen, J. (2024). Depth-dependent responses of soil organic carbon under nitrogen deposition. *Global Change Biology*, *30*, e17247. https://doi.org/10.1111/gcb.17247

Hu, Z., Delgado-Baquerizo, M., Fanin, N., Chen, X., Zhou, Y., Du, G., Hu, F., Jiang, L., Hu, S., & Liu, M. (2024). Nutrient-induced acidification modulates soil biodiversity-function relationships. *Nature Communications*, *15*, 2858. https://doi.org/10.1038/s41467-024-47323-3

Huang, W., Kuzyakov, Y., Niu, S., Luo, Y., Sun, B., Zhang, J., & Liang, Y. (2023). Drivers of microbially and plant-derived carbon in topsoil and subsoil. *Global Change Biology*, *29*, 6188–6200. https://doi.org/10.1111/gcb.16951

Janssens, I. A., Dieleman, W., Luyssaert, S., Subke, J. A., Reichstein, M., Ceulemans, R., Ciais, P., Dolman, A. J., Grace, J., Matteucci, G., Papale, D., Piao, S. L., Schulze, E. D., Tang, J., & Law, B. E. (2010). Reduction of forest soil respiration in response to nitrogen

deposition. *Nature Geoscience*, *3*, 315–322. https://doi.org/10.1038/ngeo844

Jiao, S., Qi, J., Jin, C., Liu, Y., Wang, Y., Pan, H., Chen, S., Liang, C., Peng, Z., Chen, B., Qian, X., & Wei, G. (2022). Core phylotypes enhance the resistance of soil microbiome to environmental changes to maintain multifunctionality in agricultural ecosystems. *Global Change Biology*, *28*, 6653–6664. https://doi.org/10.1111/gcb.16387

Jílková, V., Devetter, M., Al Haj Ishak Al Ali, R., Angel, R., Angst, G., Jandová, K., Libra, M., & Starý, J. (2025). Tree species and soil depth affect microbial necromass contribution to soil organic matter in temperate forest soils, surpassing the impact of microbial and faunal community composition. *Functional Ecology*, *39*, 2219–2233. https://doi.org/10.1111/1365-2435.70111

Joergensen, R. G. (2018). Amino sugars as specific indices for fungal and bacterial residues in soil. *Biology and Fertility of Soils*, *54*, 559–568. https://doi.org/10.1007/s00374-018-1288-3

Kaiser, C., Franklin, O., Dieckmann, U., & Richter, A. (2014). Microbial community dynamics alleviate stoichiometric constraints during litter decay. *Ecology Letters*, *17*, 680–690. https://doi.org/10.1111/ele.12269

Kallenbach, C. M., Frey, S. D., & Grandy, A. S. (2016). Direct evidence for microbial-derived soil organic matter formation and its ecophysiological controls. *Nature Communications*, *7*, 13630. https://doi.org/10.1038/ncomms13630

Kiem, R., & Kögel-Knabner, I. (2003). Contribution of lignin and polysaccharides to the refractory carbon pool in C-depleted arable soils. *Soil Biology and Biochemistry*, *35*, 101–118. https://doi.org/10.1016/S0038-0717(02)00242-0

Knorr, M. A., Contosta, A. R., Morrison, E. W., Muratore, T. J., Anthony, M. A., Stoica, I., Geyer, K. M., Simpson, M. J., & Frey, S. D. (2024). Unexpected sustained soil carbon flux in response to simultaneous warming and nitrogen enrichment compared with single factors alone. *Nature Ecology & Evolution*, *8*, 2277–2285. https://doi.org/10.1038/s41559-024-02546-x

Kösters, R., Du Preez, C. C., & Amelung, W. (2018). Lignin dynamics in secondary pasture soils of the south African Highveld. *Geoderma*, *319*, 113–121. https://doi.org/10.1016/j.geoderma.2017.12.028

Lalonde, K., Mucci, A., Ouellet, A., & Gelinas, Y. (2012). Preservation of organic matter in sediments promoted by iron. *Nature*, *483*, 198–200. https://doi.org/10.1038/nature10855

Langmead, B., & Salzberg, S. L. (2012). Fast gapped-read alignment with bowtie 2. *Nature Methods*, *9*, 357–359. https://doi.org/10.1038/nmeth.1923

Lavallee, J. M., Soong, J. L., & Cotrufo, M. F. (2020). Conceptualizing soil organic matter into particulate and mineral-associated forms to address global change in the 21st century. *Global Change Biology*, *26*, 261–273. https://doi.org/10.1111/gcb.14859

Li, H., Yang, S., Semenov, M. V., Yao, F., Ye, J., Bu, R., Ma, R., Lin, J., Kurganova, I., Wang, X., Deng, Y., Kravchenko, I., Jiang, Y., & Kuzyakov, Y. (2021). Temperature sensitivity of SOM decomposition is linked with a K-selected microbial community. *Global Change Biology*, *27*, 2763–2779. https://doi.org/10.1111/gcb.15593

Li, X., Fu, H., Guo, D., Li, X., & Wan, C. (2010). Partitioning soil respiration and assessing the carbon balance in a *Setaria italica* (L.) *Beauv*. Cropland on the Loess Plateau, northern China. *Soil Biology and Biochemistry*, *42*, 337–346. https://doi.org/10.1016/j.soilbio.2009.11.013

Li, Y., Zhang, W., Li, J., Zhou, F., Liang, X., Zhu, X., He, H., & Zhang, X. (2023). Complementation between microbial necromass and plant debris governs the long-term build-up of the soil organic carbon pool in conservation agriculture. *Soil Biology and Biochemistry*, *178*, 108963. https://doi.org/10.1016/j.soilbio.2023.108963

Liang, C., Amelung, W., Lehmann, J., & Kästner, M. (2019). Quantitative assessment of microbial necromass contribution to soil organic matter. *Global Change Biology*, *25*, 3578–3590. https://doi.org/10.1111/gcb.14781

Liang, C., Schimel, J. P., & Jastrow, J. D. (2017). The importance of anabolism in microbial control over soil carbon storage. *Nature Microbiology*, *2*, 17105. https://doi.org/10.1038/nmicrobiol.2017.105

Liao, H., Hao, X., Qin, F., Delgado-Baquerizo, M., Liu, Y., Zhou, J., Cai, P., Chen, W., & Huang, Q. (2022). Microbial autotrophy explains large-scale soil CO_2 fixation. *Global Change Biology*, *29*, 231–242. https://doi.org/10.1111/gcb.16452

Liu, F., Qin, S., Fang, K., Chen, L., Peng, Y., Smith, P., & Yang, Y. (2022). Divergent changes in particulate and mineral-associated organic carbon upon permafrost thaw. *Nature Communications*, *13*, 5073. https://doi.org/10.1038/s41467-022-32681-7

Liu, Y., Yang, Y., Deng, Y., & Peng, Y. (2025). Long-term ammonium nitrate addition strengthens soil microbial cross-trophic interactions in a Tibetan alpine steppe. *Ecology*, *106*, e70057. https://doi.org/10.1002/ecy.70057

Liu, Y., Zou, X., Chen, H. Y. H., Delgado-Baquerizo, M., Wang, C., Zhang, C., & Ruan, H. (2023). Fungal necromass is reduced by intensive drought in subsoil but not in topsoil. *Global Change Biology*, *29*, 7159–7172. https://doi.org/10.1111/gcb.16978

Liu, Z., Zhao, C., Zhang, N., Wang, J., Li, Z., Uwiragiye, Y., Fallah, N., Crowther, T. W., Huang, Y., Huang, Y., Xu, Y., Zhang, S., Kuzyakov, Y., Siddique, K. H. M., Jia, Z., Cai, Z., Chang, S. X., Xu, M., Müller, C., & Cheng, Y. (2025). Degradable film mulching increases soil carbon sequestration in major Chinese dryland agroecosystems. *Nature Communications*, *16*, 5029. https://doi.org/10.1038/s41467-025-60036-5

Lu, J., Breitwieser, F. P., Thielen, P., & Salzberg, S. L. (2017). Bracken: Estimating species abundance in metagenomics data. *PeerJ Computer Science*, *3*, e104. https://doi.org/10.7717/peerj-cs.104

Luo, Y., Xiao, M., Yuan, H., Liang, C., Zhu, Z., Xu, J., Kuzyakov, Y., Wu, J., Ge, T., & Tang, C. (2021). Rice rhizodeposition promotes the build-up of organic carbon in soil via fungal necromass. *Soil Biology & Biochemistry*, *160*, 108345. https://doi.org/10.1016/j.soilbio.2021.108345

Ma, L., Ju, Z., Fang, Y., Vancov, T., Gao, Q., Wu, D., Zhang, A., Wang, Y., Hu, C., Wu, W., & Du, Z. (2022). Soil warming and nitrogen addition facilitates lignin and microbial residues accrual in temperate agroecosystems. *Soil Biology and Biochemistry*, *170*, 108693. https://doi.org/10.1016/j.soilbio.2022.108693

Ma, T., Zhu, S., Wang, Z., Chen, D., Dai, G., Feng, B., Su, X., Hu, H., Li, K., Han, W., Liang, C., Bai, Y., & Feng, X. (2018). Divergent accumulation of microbial necromass and plant lignin components in grassland soils. *Nature Communications*, *9*, 3480. https://doi.org/10.1038/s41467-018-05891-1

Ma, X., Wang, T., Shi, Z., Chiariello, N. R., Docherty, K., Field, C. B., Gutknecht, J., Gao, Q., Gu, Y., Guo, X., Hungate, B. A., Lei, J., Niboyet, A., Le Roux, X., Yuan, M., Yuan, T., Zhou, J., & Yang, Y. (2022). Long-term nitrogen deposition enhances microbial capacities in soil carbon stabilization but reduces network complexity. *Microbiome*, *10*, 112. https://doi.org/10.1186/s40168-022-01309-9

Neff, J. C., Townsend, A. R., Gleixner, G., Lehman, S. J., Turnbull, J., & Bowman, W. D. (2002). Variable effects of nitrogen additions on the stability and turnover of soil carbon. *Nature*, *419*, 915–917. https://doi.org/10.1038/nature01136

Niu, D., Yuan, X., Cease, A. J., Wen, H., Zhang, C., Fu, H., & Elser, J. J. (2018). The impact of nitrogen enrichment on grassland ecosystem stability depends on nitrogen addition level. *Science of the Total Environment*, *618*, 1529–1538. https://doi.org/10.1016/j.scitotenv.2017.09.318

Pastore, M. A., Hobbie, S. E., & Reich, P. B. (2021). Sensitivity of grassland carbon pools to plant diversity, elevated CO_2, and soil nitrogen addition over 19 years. *Proceedings of the National Academy of Sciences of the United States of America*, *118*, e2016965118. https://doi.org/10.1073/pnas.2016965118

Peng, Z., van der Heijden, M. G. A., Liu, Y., Li, X., Pan, H., An, Y., Gao, H., Qi, J., Gao, J., Qian, X., Tiedje, J. M., Wei, G., & Jiao, S. (2025). Agricultural subsoil microbiomes and functions exhibit lower resistance to global change than topsoils in Chinese agroecosystems. *Nature Food*, *6*, 375–388. https://doi.org/10.1038/s43016-024-01106-7

Prommer, J., Walker, T. W. N., Wanek, W., Braun, J., Zezula, D., Hu, Y., Hofhansl, F., & Richter, A. (2020). Increased microbial growth, biomass, and turnover drive soil organic carbon accumulation at higher plant diversity. *Global Change Biology*, *26*, 669–681. https://doi.org/10.1111/gcb.14777

Qiu, W., Hu, W., Curtin, D., & Motoi, L. (2021). Soil particle size range correction for improved calibration relationship between the laser-diffraction method and sieve-pipette method. *Pedosphere*, *31*, 134–144. https://doi.org/10.1016/S1002-0160(20)60055-8

Rousk, J., Baath, E., Brookes, P. C., Lauber, C. L., Lozupone, C., Caporaso, J. G., Knight, R., & Fierer, N. (2010). Soil bacterial and fungal communities across a pH gradient in an arable soil. *The ISME Journal*, *4*, 1340–1351. https://doi.org/10.1038/ismej.2010.58

Rowley, M. C., Grand, S., & Verrecchia, É. P. (2018). Calcium-mediated stabilisation of soil organic carbon. *Biogeochemistry*, *137*, 27–49. https://doi.org/10.1007/s10533-017-0410-1

Schmidt, M. W. I., Torn, M. S., Abiven, S., Dittmar, T., Guggenberger, G., Janssens, I. A., Kleber, M., Kögel-Knabner, I., Lehmann, J., Manning, D. A. C., Nannipieri, P., Rasse, D. P., Weiner, S., & Trumbore, S. E. (2011). Persistence of soil organic matter as an ecosystem property. *Nature*, *478*, 49–56. https://doi.org/10.1038/nature10386

Schuur, E. A. G., McGuire, A. D., Schädel, C., Grosse, G., Harden, J. W., Hayes, D. J., Hugelius, G., Koven, C. D., Kuhry, P., Lawrence, D. M., Natali, S. M., Olefeldt, D., Romanovsky, V. E., Schaefer, K., Turetsky, M. R., Treat, C. C., & Vonk, J. E. (2015). Climate change and the permafrost carbon feedback. *Nature*, *520*, 171–179. https://doi.org/10.1038/nature14338

Sinsabaugh, R. L., Turner, B. L., Talbot, J. M., Waring, B. G., Powers, J. S., Kuske, C. R., Moorhead, D. L., & Follstad Shah, J. J. (2016). Stoichiometry of microbial carbon use efficiency in soils. *Ecological Monographs*, *86*, 172–189. https://doi.org/10.1890/15-2110.1

Sokol, N. W., Slessarev, E., Marschmann, G. L., Nicolas, A., Blazewicz, S. J., Brodie, E. L., Firestone, M. K., Foley, M. M., Hestrin, R., Hungate, B. A., Koch, B. J., Stone, B. W., Sullivan, M. B., Zablocki, O., Trubl, G., McFarlane, K., Stuart, R., Nuccio, E., Weber, P., … Consortium, L. S. M. (2022). Life and death in the soil microbiome: How ecological processes influence biogeochemistry. *Nature Reviews Microbiology*, *20*, 415–430. https://doi.org/10.1038/s41579-022-00695-z

Takele, L., Yang, S., Chen, Z., Yuan, J., & Ding, W. (2025). Contribution of microbial necromass to soil organic carbon in profile depths exhibited opposite patterns across ecosystems: A global meta-analysis. *Soil Biology and Biochemistry*, *207*, 109842. https://doi.org/10.1016/j.soilbio.2025.109842

Tapia-Torres, Y., Elser, J. J., Souza, V., & García-Oliva, F. (2015). Ecoenzymatic stoichio-metry at the extremes: How microbes cope in an ultra-oligotrophic desert soil. *Soil Biology & Biochemistry*, *87*, 34–42. https://doi.org/10.1016/j.soilbio.2015.04.007

Tedersoo, L., Mikryukov, V., Zizka, A., Bahram, M., Hagh-Doust, N., Anslan, S., Prylutskyi, O., Delgado-Baquerizo, M., Maestre, F. T., Pärn, J., Öpik, M., Moora, M., Zobel, M., Espenberg, M., Mander, Ü., Khalid, A. N., Corrales, A., Agan, A., Vasco-Palacios, A.-M., … Abarenkov, K. (2022). Global patterns in endemicity and vulnerability of soil fungi. *Global Change Biology*, *28*, 6696–6710. https://doi.org/10.1111/gcb.16398

Vance, E. D., Brookes, P. C., & Jenkinson, D. S. (1987). An extraction method for measuring soil microbial biomass C. *Soil Biology and Biochemistry*, *19*, 703–707. https://doi.org/10.1016/0038-0717(87)90052-6

Wang, B., An, S., Liang, C., Liu, Y., & Kuzyakov, Y. (2021). Microbial necromass as the source of soil organic carbon in global ecosystems. *Soil Biology & Biochemistry*, *162*, 108422. https://doi.org/10.1016/j.soilbio.2021.108422

Wang, B., Huang, Y., Li, N., Yao, H., Yang, E., Soromotin, A. V., Kuzyakov, Y., Cheptsov, V., Yang, Y., & An, S. (2022). Initial soil formation by biocrusts: Nitrogen demand and clay protection control microbial necromass accrual and recycling. *Soil Biology and Biochemistry*, *167*, 108607. https://doi.org/10.1016/j.soilbio.2022.108607

Whalen, E. D., Grandy, A. S., Sokol, N. W., Keiluweit, M., Ernakovich, J., Smith, R. G., & Frey, S. D. (2022). Clarifying the evidence for microbial- and plant-derived soil organic matter, and the path towards a more quantitative understanding. *Global Change Biology*, *28*, 7167–7185. https://doi.org/10.1111/gcb.16413

Wilson, C. H., Strickland, M. S., Hutchings, J. A., Bianchi, T. S., & Flory, S. L. (2018). Grazing enhances belowground carbon allocation, microbial biomass, and soil carbon in a subtropical grassland. *Global Change Biology*, *24*, 2997–3009. https://doi.org/10.1111/gcb.14070

Xing, A., Du, E., Shen, H., Xu, L., de Vries, W., Zhao, M., Liu, X., & Fang, J. (2022). Nonlinear responses of ecosystem carbon fluxes to nitrogen deposition in an old-growth boreal forest. *Ecology Letters*, *25*, 77–88. https://doi.org/10.1111/ele.13906

Xu, J., Wang, Y., Zhang, Y., Li, Q., Du, B., Asitaiken, J. L. H. T., Liu, Y., Niu, D., Fu, H., & Yuan, X. (2024). Effect of nitrogen addition on soil net nitrogen mineralization in topsoil and subsoil regulated by soil microbial properties and mineral protection: Evidence from a long-term grassland experiment. *Science of the Total Environment*, *947*, 174686. https://doi.org/10.1016/j.scitotenv.2024.174686

Yang, L., Canarini, A., Zhang, W., Lang, M., Chen, Y., Cui, Z., Kuzyakov, Y., Richter, A., Chen, X., Zhang, F., & Tian, J. (2024). Microbial life-history strategies mediate microbial carbon pump efficacy in response to N management depending on stoichiometry of microbial demand. *Global Change Biology*, *30*, e17311. https://doi.org/10.1111/gcb.17311

Ye, C., Chen, D., Hall, S. J., Pan, S., Yan, X., Bai, T., Guo, H., Zhang, Y., Bai, Y., & Hu, S. (2018). Reconciling multiple impacts of nitrogen enrichment on soil carbon: Plant, microbial and geochemical controls. *Ecology Letters*, *21*, 1162–1173. https://doi.org/10.1111/ele.13083

Yuan, M. M., Guo, X., Wu, L., Zhang, Y., Xiao, N., Ning, D., Shi, Z., Zhou, X., Wu, L., Yang, Y., Tiedje, J. M., & Zhou, J. (2021). Climate warming enhances microbial network complexity and stability. *Nature Climate Change*, *11*, 343–348. https://doi.org/10.1038/s41558-021-00989-9

Yuan, X. (2026). Data from: Depth-dependent mechanisms regulate accumulation of plant- and microbial-derived residues under long-term nitrogen addition in a semiarid grassland. *Dryad Digital Repository*. https://doi.org/10.5061/dryad.866t1g25j

Yuan, X., Niu, D., Gherardi, L. A., Liu, Y., Wang, Y., Elser, J. J., & Fu, H. (2019). Linkages of stoichiometric imbalances to soil microbial respiration with increasing nitrogen addition: Evidence from a long-term grassland experiment. *Soil Biology and Biochemistry*, *138*, 107580. https://doi.org/10.1016/j.soilbio.2019.107580

Yuan, X., Niu, D., Guo, D., & Fu, H. (2023). Responses of soil carbon and nitrogen mineralization to nitrogen addition in a semiarid grassland: The role of season. *Catena*, *220*, 106719. https://doi.org/10.1016/j.catena.2022.106719

Yuan, X., Niu, D., Wang, Y., Boydston, A., Guo, D., Li, X., Wen, H., Qin, Y., & Fu, H. (2019). Litter decomposition in fenced and grazed grasslands: A test of the home-field advantage hypothesis. *Geoderma*, *354*, 113876. https://doi.org/10.1016/j.geoderma.2019.07.034

Yuan, X., Niu, D., Weber-Grullon, L., & Fu, H. (2020). Nitrogen deposition enhances plant-microbe interactions in a semiarid grassland: The role of soil physicochemical properties. *Geoderma*, *373*, 114446. https://doi.org/10.1016/j.geoderma.2020.114446

Zeng, X.-M., Feng, J., Yu, D.-L., Wen, S.-H., Zhang, Q., Huang, Q., Delgado-Baquerizo, M., & Liu, Y.-R. (2022). Local temperature increases reduce soil microbial residues and carbon stocks. *Global Change Biology*, *28*, 6433–6445. https://doi.org/10.1111/gcb.16347

Zhang, X., & Amelung, W. (1996). Gas chromatographic determination of muramic acid, glucosamine, mannosamine, and galactosamine in soils. *Soil Biology and Biochemistry*, *28*, 1201–1206. https://doi.org/10.1016/0038-0717(96)00117-4

Zhang, Y., Niu, D., Li, Q., Liu, H., Wang, Y., Xu, J., Du, B., Guo, D., Liu, Y., Fu, H., & Yuan, X. (2025). Nonlinear response of soil microbial network complexity to long-term nitrogen addition in a semiarid grassland: Implications for soil carbon processes. *Agriculture, Ecosystems & Environment*, *380*, 109407. https://doi.org/10.1016/j.agee.2024.109407

Zhang, Y., Wang, Y., Zhou, G., Revillini, D., Liu, H., Wu, S., Chen, N., Du, B., Xu, J., Li, Q., Guo, D., Delgado-Baquerizo, M., Niu, D., Fu, H., & Yuan, X. (2025). Soil microbial networks mediate long-term effects of nitrogen fertilization on ecosystem multiservices. *Journal of Ecology*, *00*, 1–20. https://doi.org/10.1111/1365-2745.70112

Zhou, Z., Wang, C., & Luo, Y. (2020). Meta-analysis of the impacts of global change factors on soil microbial diversity and functionality. *Nature Communications*, *11*, 3072. https://doi.org/10.1038/s41467-020-16881-7

Zou, Z., Ma, L., Wang, X., Chen, R., Jones, D. L., Bol, R., Wu, D., & Du, Z. (2023). Decadal application of mineral fertilizers alters the molecular composition and origins of organic matter in particulate and mineral-associated fractions. *Soil Biology and Biochemistry*, *182*, 109042. https://doi.org/10.1016/j.soilbio.2023.109042

SUPPORTING INFORMATION

Additional supporting information can be found online in the Supporting Information section at the end of this article.

Table S1. Details of soil microbial network topological attributes for each main ecological cluster.

Table S2. Classification of potential copiotrophs (*r*-strategists) and oligotrophs (*K*-strategists) associated bacterial/fungal taxa in this study.

Table S3. Microbial functional genes and their KO number, and corresponding enzyme involved carbon degradation detected in this study.

Table S4. Model comparisons for three types of relationships of lignin phenols with their potential predictors in the topsoil.

Table S5. Model comparisons for three types of relationships of lignin phenols with their potential predictors in the subsoil.

Table S6. Model comparisons for three types of relationships of amino sugars with their potential predictors in the topsoil.

Table S7. Model comparisons for three types of relationships of amino sugars with their potential predictors in the subsoil.

Table S8. Responses of plant properties, edaphic conditions, mineral properties and microbial diversity to increasing N addition in topsoil and subsoil.

Table S9. *F*-ratios and significant levels of the two-way ANOVAS for plant properties, edaphic conditions, mineral properties and microbial diversity quantified in two soil depth following N addition treatments.

Table S10. *F*-ratios and significant levels of the two-way ANOVAS for microbial *K*-/*r*-strategy ratio quantified in two soil depth following N addition treatments.

Figure S1. Regressions between module abundances and N addition gradients in topsoil (a–d) and subsoil (e–g). Fitted lines depict linear or quadratic functions with the 95% confidence intervals (shaded section).

Figure S2. Responses of the relative abundance of carbon degradation genes to increasing N addition in topsoil and subsoil. Solid line within each box represents the median, solid grey dot within each box represents the mean, the lower and upper hinges represent the 25th and 75th percentiles, and whiskers represent error at 10th and 90th percentiles at each N addition treatment. Different lowercase letters above the boxes denote significant differences among N addition treatments based on *Duncan's* post hoc test at the level of $p < 0.05$. N, N addition; D, soil depth; N×D, interaction of N addition and soil depth.

Figure S3. Effects of N addition on contents of soil organic carbon (SOC) (a), lignin phenols (b) and amino sugars (c) in the topsoil and subsoil. Error bars represent the mean value (±SE) for each treatment ($n = 5$). Different lowercase letters above the error bars indicate significant differences among N addition treatments, as determined by *Duncan's* post hoc test at $p < 0.05$. N, N addition; D, soil depth; N×D, interaction of N addition and soil depth.

Figure S4. Effects of N addition on relative proportion of lignin phenol constituents (a, b) and amino sugar constituents (c, d) in the topsoil and subsoil. Error bars represent the mean value (±SE) for each treatment ($n = 5$). Different lowercase letters above the error bars indicate significant differences among N addition treatments, as determined by *Duncan's* post hoc test at $p < 0.05$.

Figure S5. Relative abundances of specific fungal taxa in responses to increasing N addition gradient in topsoil and subsoil. Fitted lines depict linear or quadratic functions with the 95% confidence intervals (shaded section).

Figure S6. Relative abundances of specific bacterial taxa in responses to increasing N addition gradient in topsoil and subsoil. Fitted lines depict linear or quadratic functions with the 95% confidence intervals (shaded section).

Figure S7. Effects of N addition on plant above-ground biomass (a), litter biomass (b), topsoil root biomass ($Topsoil_{BGB}$, c) and subsoil root biomass ($Subsoil_{BGB}$, d). Error bars indicate the mean value (±SE) for each treatment ($n = 5$). Different lowercase letters above the error bars denote significant differences among N addition treatments based on *Duncan's* post hoc test at the level of $p < 0.05$.

Figure S8. Ratios of cinnamyl to vanillyl (C/V) versus syringyl to vanillyl (S/V) (a) and acid to aldehyde ratios of syringyl and vanillyl units $(Ac/Al)_S$ versus $(Ac/Al)_V$ (b) for lignin phenols in the topsoil and subsoil across all N addition treatments. Blue and red dashed lines represent average values in the topsoil and subsoil, respectively. ***across both dashed lines denote significant differences between topsoil and subsoil, based on a paired-sample *t* test at $p < 0.05$.

Figure S9. Effects of N addition on ratios of amino sugar to lignin phenol (amino sugar/lignin phenol) in the topsoil and subsoil. Error bars represent the mean value (±SE) for each treatment ($n = 5$). Different lowercase letters above the error bars indicate significant differences among N addition treatments, as determined by *Duncan's* post hoc test at $p < 0.05$. N, N addition; D, soil depth; N×D, interaction of N addition and soil depth.

Figure S10. Effects of N addition on microbial biomass carbon (MBC; a), microbial biomass nitrogen (MBN; b), MBC to MBN ratio (MBC/MBN; c), β-1,4-glucosidase activity(BG; d), N-acetyl-β-D-glucosaminidase + leucine aminopeptidase activity (NAG + LAP; e), (f) BG to NAG + LAP ratio (BG/NAG + LAP; f), qCO_2 (g) and carbon use efficiency (CUE; h) in the topsoil and subsoil. Error bars represent the mean value (±SE) for each treatment ($n = 5$). Different lowercase letters above the error bars indicate significant differences among N addition treatments, as determined by *Duncan's* post hoc test at $p < 0.05$. N, N addition; D, soil depth; N × D, interaction of N addition and soil depth.

Figure S11. Spearman correlation between plant-derived and microbial-derived soil organic carbon (SOC) and relatively abundant fungal and bacterial taxa in topsoil (a) and subsoil (b). * and ** are statistically significant at $p < 0.05$ and $p < 0.01$, respectively.

Figure S12. Spearman correlation between relative abundances of C degradation genes and plant properties, edaphic conditions, mineral protection, relatively abundant fungal taxa and relatively abundant bacterial taxa in topsoil (a) and subsoil (b). * and ** are statistically significant at $p < 0.05$ and $p < 0.01$, respectively. PCI, plant carbon input; DOC, dissolved organic carbon; DIN, dissolved inorganic nitrogen; TDN, total dissolved nitrogen; Ca_{exe}, exchangeable Ca^{2+}; Mg_{exe}, exchangeable Mg^{2+}; $Fe_p + Al_p$, sum of pyrophosphate-extractable Fe/Al oxides; $Fe_o + Al_o$, sum of oxalate-extractable Fe/Al oxides.

How to cite this article: Yuan, X., Yao, S., Zhou, G., Frew, A., Dietrich, P., Li, Y., Wang, Y., Ma, T., Chen, N., Zhang, Y., Xu, J., Wu, S., Zhang, M., Li, Y., Du, B., Chang, P., Han, T., Niu, D., Fu, H., & Wang, Z. (2026). Depth-dependent mechanisms regulate accumulation of plant- and microbial-derived residues under long-term nitrogen addition in a semiarid grassland. *Functional Ecology*, *00*, 1–19. https://doi.org/10.1111/1365-2435.70341